

## Oceanic Isostasy: Seafloor Spreading and Rift Localization

James A. Conder<sup>1</sup>

<sup>1</sup>School of Earth Systems and Sustainability, Southern Illinois University, Carbondale, IL, USA  
[conder@geo.siu.edu](mailto:conder@geo.siu.edu)

### Key Points:

- 1) Oceanic isostasy may be an important key to the facilitation and localization of seafloor spreading
- 2) Evidence for and influence of oceanic isostasy on seafloor spreading can be seen across the globe from rifted margins to Iceland to backarc spreading.

20 **Abstract**

21 Why Earth is the only known planet with plate tectonics is a long-standing question. The primary  
22 driving forces of plate tectonics are widely understood to entail slab-pull, ridge-push, and mantle  
23 basal tractions. Mantle tractions are usually understood in terms of active upwellings within the  
24 mantle convective system, but such upwelling are fraught with difficulties in sustaining long  
25 term continuity with the overriding plates. Recognition that basal tractions can be modified by  
26 the isostatic response of thermal subsidence in the presence of an overlying ocean may reconcile  
27 the difficulties. In particular, greater thermal subsidence near the ridge axis, requires a systematic  
28 outward mass flux beneath the plate to maintain gravitational equilibrium. This flow biases basal  
29 tractions from resistance to plate push. This outward directed flow gives the plate a perpetual  
30 resistance-free base facilitating self-sustaining plate separation and boundary localization.  
31 Localization of the plate boundary can explain why oceanic boundaries tend to narrow in  
32 comparison to subaerial boundaries. Oceanic isostasy has likely impacted tectonics from Iceland  
33 to backarc spreading to the continental slivers dotting the oceans. That the ocean plays an  
34 integral part to perpetuating seafloor spreading may be an important puzzle piece as to why only  
35 Earth exhibits plate tectonics.

36  
37  
38

39 **1 Introduction**

40 To some degree, plate tectonics is a surface manifestation of underlying mantle dynamics  
41 (Bercovici et al., 2000; Coltice et al., 2017). That plate tectonics is only known to occur on Earth  
42 suggests something fundamentally different about the Earth's mantle dynamics than other  
43 terrestrial planets (Martin et al., 2008). An important key to the perpetuation of plate tectonics on  
44 a planet is the how and why of self-sustaining continuous generation of new seafloor at a  
45 spreading axis.

46  
47 Seafloor spreading poses a bit of a paradox. Seafloor spreading seems a nearly ubiquitous  
48 process in the geological record. Seafloor spreading has been active on Earth for perhaps three  
49 billion years or more (Cawood et al., 2018). It is responsible for the creation of majority of  
50 Earth's surface and an integral part of Earth's current dynamics (Cramer et al., 2019). Earth's  
51 supercontinents have come together and ruptured apart multiple times in Earth's history (Nance  
52 and Murphy, 2013). Rifted margins of widely varying structure evolve to spreading (Perez-  
53 Gussinye et al., 2023; Sapin et al., 2021), sometimes quickly (Umhoefer, 2011; Wang et al.,  
54 2019) and with rapid along strike propagation (Taylor et al., 1995).

55  
56 Simultaneously, seafloor spreading has been fairly difficult to account for. Despite rift structures  
57 on virtually all terrestrial planets, no other known planet exhibits seafloor spreading (Martin et  
58 al., 2008). The forces required to rupture continental lithosphere do not present a simple pathway  
59 to evolve to spreading (Brune et al., 2023; Buck, 2007). Failed rifts, like the Mid-continent rift in  
60 North America (Ojakangas et al., 2001; Stein et al., 2018) and the West African Rift System  
61 (Ghoms et al., 2022) are of size and magmatic output comparable or exceeding other rifts that

62 did transition to spreading. Even some rifted margins that did transition, such as the north central  
63 Atlantic took remarkably long time to fully rupture after initial rifting (Worthington et al., 2021).

64  
65 Suggested answers to the question as to why Earth has plate tectonics include large  
66 extraterrestrial impacts such as the one that created the moon (O'Neill et al., 2017), plume  
67 activity (Gerya et al., 2015), and the presence of water in the mantle (Bercovici, 1998; Dymkova  
68 and Gerya, 2013; Regenauer-Lieb et al., 2001; van der Lee et al., 2008). The importance of water  
69 in facilitating plate tectonics has been identified as affecting the rheology of the mantle and crust,  
70 likely contributing to development of both a weak asthenosphere and enhancing deformation at  
71 plate boundaries (e.g., Bercovici, 1998). Additionally, water can enhance faulting by lubrication  
72 and increasing pore pressures (Dymkova and Gerya, 2013). While potentially each are important  
73 factors, here I look at another direct effect of water - specifically the overlying ocean - in  
74 facilitating and localizing seafloor spreading by inducing basal tractions aligned with spreading.

75

## 76 **2 Plate driving forces**

77 The energy behind plates moving on the planet ultimately derives from heat and gravity. The  
78 first viable connection between mobile continents and planetary forces mobilizing them was  
79 made in the first half of the 20<sup>th</sup> century by Arthur Holmes (Holmes, 1931) in what he termed  
80 'substratum convection' - mantle convection as we now know it. His real genius was  
81 demonstrating how a planetary heat engine could produce horizontal forces from essentially  
82 vertical dynamics. This remains the central condition of all plate tectonic forces where  
83 gravitational instabilities result in horizontal forces.

84

85 The primary forces driving plate tectonics are some combination of ridge push, slab pull, and  
86 mantle tractions (Becker and O'Connell, 2001; Coltice et al., 2019; Forsyth and Uyeda, 1975),  
87 again horizontal forces arising from gravitational instabilities. Considerable evidence points to  
88 slab pull as being a dominant force (Conrad and Lithgow-Bertelloni, 2002; Forsyth and Uyeda,  
89 1975), although plate motions must already be developed to some degree prior to subduction  
90 initiation. The magnitude of ridge push is smaller than slab pull by roughly an order of  
91 magnitude (e.g., Fowler et al., 1990). It is a force that arises with the difference in elevation  
92 across a plate and varies by plate age as elevation differences increase; Young plates (< 5 Myr)  
93 have forces  $\sim 10^{11}$  N/m with values increasing to  $> 10^{12}$  N/m for plates older than  $\sim 25$  Myr. Of  
94 course, while ridge push increases with plate growth, basal resistance over a stationary mantle  
95 also correspondingly increases. While there is broad consensus that mantle tractions are  
96 necessary in plate tectonic development (e.g., Bercovici et al., 2000), our understanding of  
97 exactly how mantle tractions participate in plate motions still has large deficiencies. For  
98 example, it takes only a cursory look at popular explanations of seafloor spreading to find  
99 graphics of large convection cells beneath diverging plates with the upwelling cell limbs aligned  
100 with the spreading center between. Besides suggesting a likely erroneous Rayleigh number of the  
101 mantle (Weeraratne and Manga, 1998), such pictures fail when considering how plates grow,  
102 shrink, and migrate. To maintain upwelling limbs beneath a migrating mid-ocean ridge and  
103 growing plate, the aspect ratios of the cells will become inconsistent with each other as well as  
104 the overlying plates; Subducting ridges would imply superimposed upwelling and downwelling  
105 limbs, etc. Still, the prevalence of such figures are likely to remain in the absence of a clear  
106 alternative relationship between underlying mantle flow and plate motion.

107

### 108 **3 Oceanic isostasy**

109 Oceanic isostasy is an only recently explored forcing function on oceanic mantle dynamics and  
110 hence mantle tractions (Conder, 2012, 2022a). One reason it has been long-overlooked is that  
111 isostasy is typically viewed as a static or transient state and does not immediately lend itself as  
112 an obvious contributor to a steady-state process like seafloor spreading. However, under certain  
113 geological conditions, isostasy can act in non-transient ways. For example, one of the pioneers in  
114 continental isostasy suggested long-term isostatically induced horizontal compression in a  
115 system like the North American eastern seaboard; The compression arising from the isostatic  
116 return mass flux ‘undertow’ as mass is continually eroded from the nearby mountains and  
117 deposited on the continental shelf (Hayford, 1911) (Figure 1). The undertow ceases only with  
118 cessation of the erosion-deposition mass redistribution.

119

120 Analogous to the process of constant return mass flux in figure 1, differential thermal subsidence  
121 of the seafloor involves a continual mass exchange at the surface as water deepens at different  
122 rates across the plate. To maintain gravitational equilibrium, this surface water mass exchange  
123 must be balanced by a deeper counter mass exchange (Figure 2). Our current geophysical  
124 understanding of thermal isostasy in the oceans largely follows the work of Parsons and Sclater  
125 (1977). The depth of the seafloor is widely understood to be controlled by Pratt isostasy resulting  
126 in the well-known depth-square root of age relationship where the mid-ocean ridge system is  
127 topographically high and seafloor subsides as it ages and moves away from the ridge due to  
128 cooling. In the decades following this seminal work, the overlying ocean has invariably been  
129 treated as a static load correction, necessary to account for the excess mass effect on the shape of

130 the seafloor (e.g., Turcotte and Schubert, 2002 section 4.22). While substantively correct with  
131 longstanding predictive power for understanding for depth of the seafloor, the Parsons and  
132 Sclater work has perhaps been a little too successful; In particular, the ocean and mantle dynamic  
133 interplay required to maintain the isostatic equilibrium that their work depends on remains  
134 almost entirely unconsidered.

135  
136 In essence, to maintain gravitational equilibrium, the flux of ocean mass towards more rapidly  
137 thermally subsiding younger seafloor must be balanced by a corresponding flux of asthenosphere  
138 mass directed towards older lithosphere. As thermal subsidence is continual and systematic, this  
139 isostatic response must likewise be continual and systematic (Figure 2). While isostatic in nature,  
140 this dynamically maintained equilibrium does not fit cleanly as either Pratt-type or Airy-type  
141 isostasy. Here I term it ‘oceanic isostasy’. The 1D analytic solution of the physics of this oceanic  
142 isostasy for a constant velocity plate is derived in Conder (2012).

143  
144 The outward directed asthenosphere flow induced from oceanic isostasy only incrementally leads  
145 the overlying lithospheric plate with tractions less than those estimated for ridge push (Conder,  
146 2012). Nonetheless, oceanic isostasy may have profound implications on the plate motions.

147 Firstly, although the forces are small in absolute terms compared to ridge push or slab pull ( $10^8$  –  
148  $10^{11}$  N/m), asthenosphere leading the lithosphere alters the plate tectonic force balance by giving  
149 a systematically positive push to the plate and supplanting what would otherwise be basal  
150 resistance. At a minimum, this gives a resistance-free base for plates to glide on allowing forces  
151 like ridge push greater efficiency. Further, because these tractions come from the isostatic  
152 response to the plate itself, the form of the self-sustaining asthenosphere flow stays aligned with

153 the plate geometry through plate growth and migration. Secondly, the outward tractions can help  
154 localize the divergent plate boundary.

155

156 While continental rifting precedes seafloor spreading, there are clear fundamental differences  
157 between the two processes. Continental rifting typically entails stretching continental crust,  
158 frequently, but not always with significant magma emplacement (Bialas et al., 2010). Continental  
159 rifts may be wider or narrower (100s of km wide vs 100km or less) (Buck, 2007). Continental  
160 rifting involves thicker crust and lithosphere than that near spreading axes. In contrast, seafloor  
161 spreading generates entirely new igneous crust (as opposed to stretching) in a more continuous  
162 fashion reflected in regular and symmetric gravity and magnetic anomalies.

163

164 The ocean has always been treated as incidental to seafloor spreading. However, the above  
165 isostatic considerations suggest that it could play an important role in facilitating plate separation  
166 during seafloor spreading. As noted above, there are fundamental differences in structure and  
167 process between continental rifting and seafloor spreading and to date the tipping point for a  
168 system to move from rifting to spreading has been elusive. Arguably, the most fundamental  
169 difference is in seafloor spreading being more continuous and self-sustaining in its behavior,  
170 reflected in systematic morphology, magnetic anomalies, gravity anomalies, and ultimately the  
171 steady-state creation of new oceanic crust. Study of rifts and rifted margins to understand the  
172 transition to spreading has led to a wealth of information about crustal behavior and evolution  
173 during extension (e.g., GeoPRISMS, 2015). However, the diversity of rifted margins in structure  
174 and strain history gives no overarching theory as to the successful tipping points of when a  
175 continental rift will transition to seafloor spreading (Brune et al., 2023).

176

177 The elimination of basal resistance that arises with thermal subsidence in the presence of an  
178 ocean may present this tipping point for the transition of continental rifting to seafloor spreading  
179 (Conder, 2022a). It has long been recognized that tractions on the base of the lithosphere are  
180 central to plate tectonics; Yet, basal tractions may be either driver or drag to plate motions  
181 depending on whether the underlying viscous mantle leads or lags the motion of the overlying  
182 plate (e.g., Forsyth and Uyeda, 1975). In mature spreading systems, forces like ridge push and  
183 slab pull likely dominate though their effectiveness is greater when basal drag is diminished. As  
184 continental rifts must be exerting forces sufficient for lithosphere extension over resistance from  
185 the lithosphere itself and from viscous basal tractions, an active rift system experiencing  
186 inundation can receive a positive push towards stable extension with the reduction in resistance  
187 that comes with the onset of isostatically driven undertow.

188

### 189 3.1 Quantitative development of oceanic isostasy

190 Drawing largely on Conder (2012), a brief sketch of the underlying physics is presented here. A  
191 useful starting point for understanding oceanic isostasy is with Pratt isostasy and the square root  
192 of age-depth equation for seafloor,

$$193 \quad d = d_{ridge} + c\sqrt{t}, \quad (1)$$

194 where  $d$  is ocean depth,  $d_{ridge}$  is ridge depth and  $t$  is seafloor age. The subsidence constant,  $c$ ,  
195 depends on several factors, including thermal expansion, mantle temperature, thermal diffusivity,  
196 mantle density at reference mantle temperature,  $\rho_m$ , and ocean density,  $\rho_w$ . Lumping properties  
197 other than densities into a constant,  $f$ , gives,

$$198 \quad c = f \frac{\rho_m}{\rho_m - \rho_w}, \quad (2)$$

199 The factor  $\rho_m / (\rho_m - \rho_w)$  accounts for the mass due to the overlying substrate. Subaerially, this  
200 factor goes to unity. Subaerial cooling is fully Pratt compensated as no mass enters or leaves  
201 with cooling and contraction. For mantle density of  $3330 \text{ kg/m}^3$  and ocean density of  $1030$   
202  $\text{kg/m}^3$ , this implies submarine subsidence 45% greater than subaerial subsidence for crust of  
203 similar age (Figure 3). As this excess 45% comes from ocean mass being continually  
204 redistributed among columns during subsidence, a mechanism other than Pratt isostasy must  
205 accommodate nearly 1/3 of the gravitational disequilibrium. Reattaining gravitational  
206 equilibrium to account for the water mass redistribution requires a counter redistribution of mass  
207 in the asthenosphere.

208

209 The amount of mass that ultimately must be redistributed from any column is equal to the excess  
210 mass,  $\gamma$ , increase arising from the overlying ocean, the difference between submarine and  
211 subaerial subsidence curves (Figure 3a). Assuming  $c_{submarine} \sim 0.35 \text{ km/Myr}^{1/2}$

$$212 \quad \gamma = \left( 0.11 \frac{\text{km}}{\text{Myr}^{1/2}} \right) \sqrt{t}. \quad (3)$$

213 As this is a continually ongoing process with previous disequilibria already adjusted for, the  
214 relevant curve to consider is the rate of mass increase (Figure 3b). Differentiating equation 3  
215 with respect to time gives the rate of mass accumulation in each column,

$$216 \quad \dot{\gamma} = 0.055 \frac{\text{km}}{\text{Myr}^{1/2}} / \sqrt{t}. \quad (4)$$

217 Because younger seafloor subsides more rapidly than older seafloor, excess is added more  
218 rapidly to young seafloor requiring a counter asthenospheric flow away from young seafloor  
219 towards older seafloor.

220

221 The change in mass in a column due to lateral asthenosphere counter flow is the mass flux into  
222 the column minus the mass flux out of the column. In 1D, the governing equation becomes,

$$223 \quad \dot{\gamma}^* - \frac{dU}{dx} = 0, \quad (5)$$

224 where,

$$225 \quad \dot{\gamma}^* = \dot{\gamma} - \dot{\gamma}_{mean}, \quad (6)$$

226 and  $U$  is the lateral asthenosphere mass flux (in units of km<sup>2</sup>/Myr). The flux as a function of  
227 position,  $U(x)$ , can be found by

$$228 \quad U(x) = \int_0^x \dot{\gamma}^* dx, \quad (7)$$

229 As shown in the supplementary material of Conder (2022a), associated basal tractions,  $\sigma$ , may be  
230 estimated by assuming  $U$  is maintained through Poiseuille flow in the asthenosphere. Given a  
231 channel width,  $H$ , and viscosity,  $\eta$ ,

$$232 \quad \sigma = 1.5\eta U/H^2. \quad (8)$$

233 To maintain consistency with the previous work, calculations of tractions in this manuscript  
234 assume  $H$  to be 100 km and  $\eta$  to be 10<sup>20</sup> Pa·s. A numerical solution is given in Conder (2022a)  
235 and maintained as a MatLab function at: [https://opensiuc.lib.siu.edu/geol\\_comp/](https://opensiuc.lib.siu.edu/geol_comp/).

236

237

#### 238 **4 Localization of spreading centers**

239 A clear difference of mid-ocean spreading centers relative to continental rifts is the narrow,  
240 stable, well-defined axis of extension giving rise to localized seismicity and a regular pattern of  
241 magnetic anomalies. While the weakest part of the plate will preferentially rupture under  
242 extension, the systematic undertow induced from oceanic isostasy may directly factor in the  
243 tighter orderliness of spreading centers. The outward mass flux centers on the locus of greatest

244 submarine subsidence (most rapid ocean deepening) (Figure 4). For most of the ridge system this  
245 is the spreading axis, so alignment of outward flow from the axis reinforces mantle tractions  
246 tending towards a single locus of extension. A quantification of localization forces can be found  
247 by integrating outward tractions as a function of location (Figure 4d). Positive values promote  
248 extension and negative values promote compression.

249

250 Even in a messy thermal state, potentially like that of a continental rift, a preferential spreading  
251 locus may develop with submergence. Figure 5 shows localization preference for an instance  
252 with two loci of rifting. Even with two loci, the basal mantle tractions give a preference for  
253 localizing at one over the other. Going further, figure 6 shows two examples of randomly  
254 distributed thermal ages (a), their associated mass fluxes arising with submergence (b), and the  
255 strength of localization across the system (c). Even with randomness in the thermal system, once  
256 submergence occurs, there are preferential loci for extension where subsequent new crust is  
257 likely to be emplaced, leading to a self-reinforcing feedback loop of raised temperatures and  
258 further localization in that place.

259

260

## 261 **5 Geological examples**

262 There are a number of areas across the globe worth examining their geophysical character and/or  
263 geological history in the context presented here. For instance, considerations could be made at  
264 rifted margins, including complex rifts like the Galicia Bank (Druet et al., 2018; Grevenmeyer et  
265 al., 2022), the Gulf of Mexico (Kneller et al., 2012), and/or backarc spreading centers.

266

267 5.1 Subaerial vs. submarine spreading

268 With its subaerial spreading, Iceland presents a unique natural test and illustration of the process  
269 at work. Extensional tectonics on the island are known to differ in substantial ways from typical  
270 seafloor spreading; Extension takes place over a broader area, dikes and earthquake swarms are  
271 common, and ridge-parallel strike-slip faulting is documented (Einarsson, 2008; Karson, 2017;  
272 Sigmundsson et al., 2020). Thicker crust (Einarsson, 2008) and/or plume processes (Karson,  
273 2017) likely contribute to these differences, but its subaerial nature may also be a contributing  
274 factor. To investigate the relative importance of the subaerial nature of extension on the island  
275 relative to thicker crust and/or hotspot processes, one can look to the portion of the spreading  
276 system that is both on-platform (thick crust) and submarine; Contrasting this section of the  
277 spreading system to adjacent submarine off-platform and subaerial on-platform sections offers a  
278 valuable examination at the relative importance of an overlying ocean on spreading center  
279 dynamics versus thicker crust and/or hotspot.

280

281 As a first order observation, ridge morphology suggests that the coastline may be at least as  
282 important of a factor in the spreading process as crustal thickness. Figure 7 shows a digital  
283 elevation model where the Reykjanes Ridge crosses the Icelandic platform and onto the island.  
284 The transition in morphology of the Reykjanes Ridge from a narrow band of en echelon  
285 spreading segments (Saemundsson et al., 2020) to the wider and more distributed volcanic zones  
286 of Iceland proper occurs across the Reykjanes Peninsula; In contrast, there is minimal response  
287 observed in the crossing from off-platform to on-platform. If the difference in morphology were  
288 primarily controlled by the structure of the platform, such as its thicker crust, the morphological  
289 differences should track with the edge of the platform rather than the coast as observed.

290 Likewise, it would be a surprising happenstance for the change to correspond tightly with the  
291 coastline if the morphology change were strictly plume-controlled.

292

293 More than just ridge morphology, changes in character of earthquake distribution, gravity and  
294 magnetic anomalies, and even the eastward shift of the plate boundary are all more tightly  
295 associated with the coastline than with the edge of the Icelandic Platform (Conder, 2022a).

296 Together these further the case that the presence of the ocean is an important factor in the  
297 observed differences. Figure 8 shows the isostatic gravity anomaly on and around the platform  
298 (Bonvalot et al., 2012). Figure 9 shows seismicity and slip vectors of extensional earthquakes  
299 from the CMT catalog (*globalcmt.org*) on and around the platform. Events are determined to be  
300 extensional, compressional, or strike-slip by the most vertical stress axis of the moment tensor:  
301 P, T, or B. Earthquakes on the submarine platform occur along a localized spreading axis and are  
302 primarily associated with normal faulting more akin to earthquakes off-platform than on the  
303 island. Across the Reykjanes peninsula events are dominated by strike-slip bookshelf faulting  
304 rather than normal faulting (Einarsson et al., 2020). Further into the island many events are  
305 associated with volcano-tectonic processes rather than simple plate separation (Einarsson, 2008),  
306 but nowhere on the island can the same coherency of extensional slip be found as on the  
307 submarine platform. Similarly, isostatic gravity anomalies have a greater change in character  
308 across the coastline than across the platform edge with anomalies on the island being less  
309 spatially coherent and showing minimal definition with the local rift axes. In virtually every  
310 geophysical dataset observed, the coastline demarcates a greater change in geophysical character  
311 than delineations expected from associations with thick crust or plume processes. The tight

312 correlation of tectonic character changes with the coastline is a strong indicator that the ocean is  
313 not passive but an active participant in the seafloor spreading process.

314

315 As Iceland is bounded by submarine regions to each side, its tectonic behavior may be subtly  
316 different than for a simple submerged/non-submerged dichotomy. Specifically, while the  
317 localization of the ridge axis for Iceland may be lacking relative to the totally submerged case in  
318 Figure 4, the mantle tractions arising around the island may be important to consider. Figure 10  
319 shows the isostatic flow response and localization for a subaerial axis with submerged flanks.  
320 Importantly, the subaerial region does not gain additional mass with thermal subsidence. The  
321 location most rapidly accumulating mass via subsidence is the submarine region just beyond the  
322 shoreline (Figure 10a). As the outward mass flux aiding seafloor spreading is not present beneath  
323 the subaerial region, the flux beneath the plateau may be directed inward (Figure 10b). If the  
324 island participates fully in the gravitational equilibrium process with the surrounding oceanic  
325 regions, localization is preferred just outside the island's edges (Figure 10d). However, if the  
326 island does not efficiently participate in the gravitational equilibration process - as the isostatic  
327 anomalies suggest (Figure 8) - localization will preferentially occur within the subaerial region,  
328 but no strong preference beyond that (figure 10e). This lack of strong localization may be why  
329 the on-island axes develop in multiple zones (figure 7) and routinely shift around the platform  
330 (Foulger et al., 2020); Similarly, informing why extensional earthquake slip vectors lose  
331 consistency on the island while maintaining consistency on the submarine platform (figure 9).

332

333 Progressing back in time, this effect of biasing extensional axes to within subaerial regions  
334 flanked by ocean may be seen in the Geological history of the Greenland-Iceland-Faroe ridge.

335 Past rift axes associated with Iceland were not restricted to the current island; Multiple former  
336 rift axes jumped around nearly the entire length of the Greenland-Faroe ridge (Foulger et al.,  
337 2020). Importantly, these rift axes were mostly subaerial at the time of their existence as the  
338 Greenland-Iceland-Faroe ridge was a land bridge until 10-15 Myr ago (Denk et al., 2011; Ellis  
339 and Stoker, 2014). As submergence of the ridge progressed, localization as seen in figure 10e  
340 likely continually constrained rift axis jumps to remaining subaerial regions – culminating in the  
341 configuration they are now.

342

## 343 5.2 Seaward dipping reflectors

344 Rifted margins are often described in terms of ‘magma-rich’ and ‘magma-poor’ end members  
345 (Franke, 2013; Peron-Pinvidic et al., 2019; Tugend et al., 2020). Magma-rich margins are  
346 typically characterized as having a package of seaward-dipping-reflectors (SDRs), frequently  
347 interpreted as thick packages of lava flows occurring during an increase of magma production  
348 associated with creation of the first oceanic crust (e.g., Chauvet et al., 2021). It may be the case  
349 that seaward dipping reflectors (SDRs) in the distal portion of the rift system are indicators of  
350 subaerial spreading (Collier et al., 2017; Jackson et al., 2000; Karner et al., 2020; Mutter et al.,  
351 1982) with analogs today in Iceland (Karner et al., 2020) and the Afar subaerial section of the  
352 Red Sea Rift (Bastow and Keir, 2011; Corti et al., 2015). Given the prevalence of magma-rich  
353 margins (e.g., Geoffroy, 2005), a high frequency of possible subaerial spreading in the geological  
354 record appears to point away from the ocean having an important role in the development of  
355 seafloor spreading. On close inspection, though, these may be exceptions that prove the rule.  
356 Despite their prevalence along the Atlantic and other margins, Iceland and Afar are the only  
357 analogs we see today; Iceland and Afar are clearly unusual in the current spreading system in

358 that 1) subaerial spreading accounts for < 1% of the current spreading system, and 2) as noted  
359 earlier, their behavior contrasts in fundamental ways with the submarine spreading system.

360

361 If distal SDRs are indicators of subaerial spreading, the intrinsic differences to seafloor spreading  
362 are important. It seems probable that without the facilitating mantle tractions, extension in  
363 Iceland and Afar are largely a kinematic response to actively facilitated spreading in the adjacent  
364 submerged plate boundary. Magma-rich in this case may indicate development of a steady state  
365 magma chamber with lithospheric thinning but without the localizing effects that come with  
366 submergence. Conspicuously, even a magma-rich region like Iceland with long-lived magma  
367 chambers appears to be largely driven by far-field tectonics as opposed to magma-driven  
368 opening (Kolzenburg et al., 2022). That magma-rich and magma-poor margins can vary over  
369 short spatial scales (Gouiza and Paton, 2017; Shillington et al., 2009) is consistent with a model  
370 of spreading tracking with inundation but with instances of Icelandic-type extension leading  
371 inundation; Spreading leading inundation may occur with adjacent inundated self-sustaining  
372 spreading centers forcing the subaerial neighbors in the system. Presumably most of these  
373 instances would evolve to stable and submerged seafloor spreading.

374

### 375 5.3 Rift to drift

376 While the number of locations where the mid-ocean ridge system crosses the coastline are  
377 limited, additional geological evidence for the ocean actively facilitating seafloor spreading can  
378 be found with the rift-to-drift transition. Places like the Afar triple junction with three  
379 extensional boundaries at different stages of the rift-to-drift transition as well as Atlantic rifted  
380 margins show the rift-to-drift transition tracking more closely with inundation than other factors

381 such as obliquity, rifting style, or even rifting intensity (Conder, 2022a). The list of locations in  
382 considering the relationship between rupture and inundation is extensive including rifted margins  
383 (Sapin et al., 2021; Unternehr et al., 2010), backarc spreading centers, and rifts on other planets.

384

385 One example to look to is rifting in the Gulf of California (GoC), a complex rifting and drifting  
386 system (Umhoefer et al., 2020) exhibiting along strike variability in rifting structures (Lizarralde  
387 et al., 2007; van Wijk et al., 2017). Extension is primarily accommodated along multiple long  
388 transform faults connecting several short spreading segments (Figure 11). Although young,  
389 seafloor spreading and extension in the GoC has a complex evolution culminating in fully  
390 developed spreading in the south and pull-apart basin extension in the north (van Wijk et al.,  
391 2017). Prior to opening, subduction of the Farallon plate occurred off the west coast of Baja  
392 California. Rifting began in Baja after the subducting plate was consumed (~12 Ma);  
393 Subsequently, the GoC captured the primary plate boundary along the previously active  
394 continental arc moving it inland (Michaud et al., 2006; Umhoefer, 2011). Rupture along the  
395 ~1500 km long system occurred rapidly, co-opting the plate boundary within 6-10 Myr after  
396 cessation of subduction (Umhoefer, 2011). While the rapid coalescence of the boundary must  
397 have had much to do with the weak arc lithosphere (Umhoefer, 2011), observed variations in  
398 along-strike extension style suggest other superposed tectonic effects at work as well, such as  
399 effects of sedimentation (Bialas and Buck, 2009), mantle fertility (Lizarralde et al., 2007), or  
400 structural styles (van Wijk et al., 2017). Of particular importance here, marine incursion in the  
401 GoC also appears to have a close relationship with the plate boundary coalescence and  
402 subsequent evolution and development of seafloor spreading (Umhoefer et al., 2018).

403

404 To first order, it is easily observed that seafloor spreading is occurring in the southern gulf which  
405 had more ready access to the sea contrasting with earlier stages of rifting occurring in the  
406 northern section. Of course, the details are more nuanced. Marine incursion occurred in the  
407 southernmost Gulf by 8-9 Ma corresponding with spreading propagation of the East Pacific Rise  
408 towards the arc into the southernmost gulf (Umhoefer et al., 2018). Marine incursion reached all  
409 the way to the Salton Trough around 6.5-6.3 Ma (Bennett et al., 2015; Umhoefer et al., 2018) at  
410 which time, the majority of the plate boundary localized in the GoC and the Guaymas basin in  
411 the central gulf fully transitioned to spreading (Umhoefer et al., 2018). Although the Salton  
412 Trough is no longer inundated, marine incursion into the trough may have occurred as late as the  
413 Pleistocene (Ross and and Jefferson, 2020). Free-air gravity anomalies suggest an isostatically  
414 coherent rifted domain bounded by subaerial flanks extending from the southern gulf to the  
415 Salton Trough (figure 11). That the gravity coherency crosses the oceanic-continental crust  
416 boundary within the gulf, but not across the coastline to either side (Figure 11b) suggests an  
417 ocean link to a similar isostatic behavior along the full GoC spreading system. Because of the  
418 narrowness of the GoC, it should be underscored that the viability of oceanic isostasy as a  
419 tectonic driver depends on load (incursion) width and strength of the lithosphere to support that  
420 load (Conder, 2022a); High-strength lithosphere and narrow loads are resistant to developing  
421 outward mantle tractions. Still, the gravity signal suggests that the entire rift system participates  
422 in the system's isostatic mass exchange.

423

424 While the Salton Trough remains a pull-apart basin, it is not wholly clear whether currently  
425 submerged northern gulf basins have recently ruptured fully to seafloor spreading or remain in  
426 pull-apart mode (Martin-Barajas et al., 2013; van Wijk et al., 2019) as thick sediments obscure

427 straightforward interpretation. In addition to obscuring the northern basins, the thick sediments  
428 of the northern gulf have been suggested to affect GoC tectonics. Thick sediments can reduce the  
429 buoyancy forces across the rift and tend to narrow rifting and aiding the rift-to-drift transition  
430 (Bialas and Buck, 2009). However, the rift-to-drift correlation with the sedimentary package in  
431 the GoC runs counter to that suggesting thermal effects may be more important (Martin-Barajas  
432 et al., 2013). While sediments are not efficient as a thermal blanket to weaken the lithosphere  
433 (Bialas and Buck, 2009), it may be that sediments will tend to smooth the thermal variations,  
434 reducing the degree of differential thermal subsidence, thereby slowing the localization from  
435 oceanic isostasy and delaying the rift-to-drift transition.

436

#### 437 5.4 Rafted continental slivers

438 Many rafted pieces of continental crust litter the world's ocean basins (Ashwal et al., 2017;  
439 Grevemeyer et al., 2022; King et al., 2020; Kumar et al., 2019; Nauret et al., 2019; Polteau et al.,  
440 2019; Santos et al., 2019; Scotchman et al., 2010). The fluid nature of the ocean can lead to rapid  
441 changes of an ocean's influence on underlying mantle tractions; In particular, rapid changes in  
442 the preferential locus of spreading can occur as the ocean recedes or advances in specific  
443 locations. Competing rifts may be inundated at different times; If a weaker rift is inundated first,  
444 it may begin to transition only to give way when a water path inundates a stronger competing  
445 second rift. For example, the Sao Paulo High presents an exception to the otherwise regular  
446 northward progression of the rift-to-drift transition in the South Atlantic (Heine et al., 2013;  
447 Moulin et al., 2010) (Figure 12). During this stall, the block comprising the rise was transferred  
448 from the African plate to the South American plate (Heine et al., 2013; Scotchman et al., 2010).  
449 It is plausible that a water path northward crossed an immature rift on the South American side

450 of the block to link to the rift system northward. As spreading matured north and south, a second  
451 water path may have inundated a rift on the African side of the block transferring the locus of  
452 extension to the other side (Conder, 2022b). It is not difficult to imagine similar scenarios for  
453 other stranded blocks of continental material following the rift-to-drift transition. While  
454 speculative for any individual location, such a process would be an expected implication of  
455 inundation playing an active role in seafloor spreading development.

456

457

#### 458 5.5 Backarc spreading

459 While the GoC is a former backarc evolved to spreading system, many current backarcs also  
460 have developed spreading (Martinez et al., 2007). Back-arc spreading presents a curious  
461 condition of extension in an overall compressional environment. In general, backarcs in  
462 subduction systems can be compressional or extensional with extensional systems potentially  
463 developing into spreading systems. Backarc spreading commonly results from rifting of an  
464 oceanic volcanic arc that generates and migrates into a backarc basin (Martinez and Taylor,  
465 2003). The difference in systems with backarc extension and compression have long been  
466 couched in terms of low-stress (extensional) ‘Marianas’ type and high-stress (compressional)  
467 ‘Chilean’ type subduction with high-stress more typical for continental arcs and low-stress more  
468 frequent for oceanic arcs (e.g., Uyeda, 1987). The variability in subduction and backarc systems  
469 has led to considerations of multiple variables to explain the differences such as slab dip (Bott et  
470 al., 1989) or sediment thickness (Cloos and Shreve, 1996); More refined distinctions such as  
471 accretionary vs erosional margins (e.g., Harris et al., 2014) or tsunamigenic vs non-tsunamigenic  
472 (e.g., Bilek and Lay, 2018) have been further advanced. The mechanisms driving the

473 development of backarc spreading are likewise varied in the literature (Goes et al., 2017; Heuret  
474 and Lallemand, 2005; Martinez and Taylor, 2006; Sdrolias and Muller, 2006; Wallace et al.,  
475 2005). Still, it is clear that extensional backarc basins dominate the oceans while compressional  
476 backarcs are more prevalent in continental regions (Heuret and Lallemand, 2005). While  
477 admittedly appearing somewhat tautological, the presence of ocean in oceanic backarcs may be a  
478 contributing factor to the development of backarc spreading.

479  
480 An ocean-ocean subduction zone in particular presents a geometrical layout favorable to active  
481 mantle tractions for facilitating spreading. The arc presents a strip of crust with thinned  
482 lithosphere and elevated temperatures (Ha et al., 2020) and high heat flow (e.g., Von Herzen et  
483 al., 2001) and therefore differential thermal subsidence. For largely submerged arc-backarc  
484 systems such as the Marianas (Figure 13a), Tonga (Taylor et al., 1996), or South Sandwich (Leat  
485 et al., 2016) this differential subsidence will tend to drive flow outward into the backarc away  
486 from the arc; Direct loading of volcanic deposits will add to the isostatic response, although  
487 likely in transient pulses. The resultant mantle tractions will augment existing tensional stresses  
488 in the overlying plate and tend to localize extension beneath the arc. If localization and full  
489 rupture does occur, the locus of differential subsidence will be strongest at the spreading axis  
490 (Figure 5) potentially leading to sustained spreading and migration into the backarc basin with  
491 continued crustal accretion.

492  
493 Pointedly, the rift-to-drift transition in backarc basins can be fundamentally different than on  
494 continental rifted margins (Wang et al., 2019). Inherent differences may arise in that back-arc  
495 basins typically begin in a fully submerged state, while continental rifting is frequently

496 associated with advancing inundation. Advancing inundation can invoke a transient additional  
497 push for rift opening (Conder, 2022a); Such differences may lead to inherently different opening  
498 progressions for backarcs relative to continents. For instance, rather than progressive extension  
499 leading to rupture (e.g., Brune et al., 2016; Davis and Lavier, 2017; Lavier and Manatschal,  
500 2006), backarc spreading axes are shown to intrude laterally on diffusely extending regions  
501 through propagation or synchronous jumping (Dunn et al., 2013; Taylor et al., 1995; Wang et al.,  
502 2019). That an already extensively faulted and extending region preferentially localizes along a  
503 crack originating outside the area is peculiar; The implication being that the outside propagating  
504 crack has something intrinsic to localization that the already present extensional cracks within do  
505 not. That a localized and propagating axis may have outwardly directed mantle tractions that  
506 track with its growth in contrast to faults within the area can straightforwardly account for the  
507 co-option.

508

509 The Okinawa Trough (Figure 13b) is an unusual case of backarc rifting within continental crust  
510 (Arai et al., 2017). Extension in the ~1000 km long Okinawa Trough began in the Miocene  
511 (Fournier et al., 2001). Current extension rates vary considerably along strike with ~1 cm/yr in  
512 the northern trough to ~5 cm/yr in the south (Nishimura et al., 2004). Extension is diffuse in the  
513 slower northern trough and localized along narrow axes in the central and southern trough (Arai,  
514 2021; Nishizawa et al., 2019). Such structure must be transient as continued spreading will  
515 undoubtedly create oceanic crust within the basin; Still the current literature for the rift-to-drift  
516 transition makes little allowance for the possibility of localization within continental crust prior  
517 to the transition to spreading. As this is also an unusual case of a submerged continental arc and

518 backarc, this joint occurrence may be a manifestation of the effectiveness of isostatically driven  
519 mantle tractions contributing to backarc spreading development and evolution.

520

## 521 **6 Oceanic vs. continental tectonics**

522 Notwithstanding the remarkable successes of plate tectonics in understanding the history and  
523 deformation of the Earth's crust, continental deformation only loosely adheres to the  
524 fundamental assumptions of non-deforming plate interiors and narrowly confined boundaries  
525 (England and Jackson, 1989; Molnar, 1988; Thatcher, 1995). Many plate boundaries on Earth  
526 can be classified as 'diffuse' in that they do not fit the classical definition of deformation being  
527 limited to a narrow boundary (Gordon, 1998; Stein and Sella, 2002) (Figure 14). For continents,  
528 plate boundaries frequently entail wide topographic and seismically active zones; These being  
529 the norm for both compressional (e.g., Tibetan plateau, Hindu Kush) and extensional regions  
530 (e.g., Basin and Range, portions of the East African Rift) rather than the exception (Gordon and  
531 Stein, 1992). Even 'narrow' single-valley extensional boundaries like the Main Ethiopian Rift  
532 (Corti, 2009) and Rio Grande Rift (Hudson and Grauch, 2013) are several tens of kilometers  
533 wide and 3:1 being a high length to width aspect ratio for individual basins. Continental strike  
534 slip boundaries like the San Andreas can be 100km or more wide (Bennett et al., 2002; Thatcher,  
535 1995). In contrast, oceans tend to more closely adhere to the plate tectonic assumptions of rigid  
536 interiors and narrowly confined boundaries. This dichotomy presented a large obstacle for  
537 accepting the ideas leading to plate tectonics until after the oceans began to be systematically  
538 explored in the 20th century (Sandwell, 2001). The increasing quality and quantity of geodetic  
539 data, such as GPS, repeatedly exposes more regional complexity of continental deformation; The  
540 complexity frequently requires additional microplates, tectonic blocks, or diffusely deforming

541 regions to adequately explain the data (Hasterok et al., 2022; Stamps et al., 2021; Wang and  
542 Shen, 2020). While diffuse boundaries are also recognized in the oceans (Gordon, 1998, 2023;  
543 Stein and Sella, 2002), they are of a decidedly different nature than those on continents (Figure  
544 14); Diffuse oceanic plate boundaries are more subtle, being identified primarily by kinematic  
545 closure misfits and/or a moderate number of earthquakes (Stein and Sella, 2002) and  
546 characterized by smaller strain rates than other boundary zones (Zatman and Richards, 2002).  
547 Primary examples are found in the Indian ocean (Conder and Forsyth, 2001; Royer and Gordon,  
548 1997; Wiens et al., 1985) and in the Atlantic between the North and South American plates  
549 (DeMets and Merkouriev, 2019).

550

551 The dichotomy between continental and oceanic tectonics is typically explained in terms of  
552 contrasting crustal rheologies with continental crust being thicker and often with a weak ductile  
553 layer in the lower crust (Molnar, 1988; Thatcher, 1995). While the differences in rheological  
554 profiles are undoubtedly important controls on deformation, especially for enabling deformation  
555 in the third dimension like crustal thickening (Molnar, 1988), it is worth considering whether the  
556 presence of an ocean may also play a role in the dichotomy. As discussed above, Iceland's  
557 switch from a narrowly confined boundary to wider deformation occurs at the coastline rather  
558 than the edge of the submarine platform (figure 7). For mantle tractions to localize spreading  
559 centers, there are two requirements: systematic differential subsidence (say from thermal  
560 variations) and an overlying fluid layer to redistribute mass with that differential subsidence. As  
561 diffuse oceanic boundaries do not tend to reflect major topographical or thermal variability, there  
562 is little facilitation of localizing the boundaries until rifting or some other process imposes a  
563 systematically varying thermal structure across the region.

564

565 **7 Outstanding issues**

566 The idea of oceanic isostasy as a facilitator of seafloor spreading poses potential answers to  
567 many aspects of our understanding of seafloor spreading and plate tectonics. However, it does  
568 pose several questions of its own that are currently unanswered and listed here. This list should  
569 be considered representative rather than comprehensive.

570

571 Possibly most importantly, the generated mantle tractions need to be considered within the  
572 broader system of mantle upwellings and convective circulation. The induced flow adds to the  
573 overall flow pattern, biasing mantle tractions towards positive push, but does not require the  
574 integrated flow at any given location to be in the plate spreading direction. So, other flows in the  
575 asthenosphere driven by plumes or other mechanisms may still be dominant mantle tractions  
576 when present. There are numerous places across the globe that show evidence for asthenosphere  
577 flow in opposition to plate motion directions (Behn et al., 2004; Conder et al., 2002; Conrad et  
578 al., 2007; Ghosh et al., 2013; Naliboff et al., 2009). Perhaps biasing the ‘average’ basal traction  
579 to positive is sufficient for the overall spreading system. Or perhaps, the fact that the isostatic  
580 response will happen as shallowly as possible, while convective flows may dominate more  
581 deeply keeps them from acting strongly in opposition. This will only be answered with a better  
582 understanding of the interaction of the various flows acting in the mantle.

583

584 The physics in Conder (2012) and used here for discussion assumes an axial high at the ridge  
585 axis, which is most appropriate for fast spreading centers. Slow spreading systems like the Mid-  
586 Atlantic Ridge exhibit median valleys (Small et al., 1998). Spreading from within a median

587 valley requires dynamic uplift of young crust as it moves away from the axis prior to thermally  
588 subsiding (Phipps Morgan et al., 1987), following a different form of subsidence near the ridge  
589 axis than that seen in figure 3. This different form will likely reduce the effectiveness of  
590 localization of the plate boundary. Neovolcanic zones within median valleys are typically wider  
591 than at fast spreading centers, sometimes wandering laterally or broadening to 5-10 km within  
592 the median valley (Macdonald, 1982). These variations may be due to the lessened efficiency of  
593 localization, but to what degree that derives from having rift shoulders rather than monotonic  
594 subsidence remains to be determined.

595

596 It is clear than not every inundated or submerged rift transitions to seafloor spreading. In some  
597 cases like the Gulf of Suez, it is straightforward as to why; Strong lithosphere can support a  
598 narrow overlying load precluding an isostatic response (Conder, 2022a, b). However, locations  
599 like the submerged northern Okinawa Trough have wide loads of submergence and likely  
600 moderate to low elastic thicknesses and are extending diffusely. It seems possible that the slow  
601 rates of opening (Nishimura et al., 2004) may preclude full rupture, although slower spreading  
602 systems, such as the Gakkel Ridge in the Arctic (Cochran et al., 2003) have transitioned.

603

604 It is fair to say that our understanding of the interplay of oceanic isostasy as a facilitator of  
605 horizontal plate motions is in the early stages. There are numerous outstanding questions to be  
606 addressed as well as undoubtedly many as yet unidentified research avenues understanding the  
607 process's contributions and limitations to shaping our planet.

608

609 **8 Summary points**

610 Differential thermal subsidence of the crust in the presence of an overlying ocean can induce a  
611 flow in asthenosphere to adjust for isostatic equilibration. Roughly 1/3 of oceanic plate  
612 gravitational equilibrium must be accommodated in this manner.

613

614 This self-sustained, isostatically-driven asthenosphere flow is directed outward from the  
615 thermally youngest (and most rapidly subsiding) part of the system, and may be a necessary  
616 component to the occurrence of seafloor spreading.

617

618 Mantle tractions induced by oceanic isostasy may lead to highly localized extension in contrast  
619 to less localized subaerial extension.

620

621 Subaerial spreading is different than submarine spreading in that it is not self-perpetuating nor  
622 may have a strongly localized boundary; Instead subaerial spreading is likely propelled along by  
623 the neighboring spreading system. Although less smooth than seafloor spreading, continual  
624 regular extension may be enough to sustain a steady-state magma chamber.

625

626 Extensional modes on Iceland contrast more strongly across the coastline than seen across the  
627 off-on platform transition or any other closed contour on the island. The coastline acting as the  
628 most prominent transition line illustrates a direct impact of the overlying ocean layer on  
629 facilitating self-perpetuating, localized seafloor spreading.

630

631 In addition to potentially facilitating seafloor spreading, oceanic isostasy may play important  
632 roles in development of other seafloor processes such as backarc opening and the existence of  
633 stranded continental slivers in the oceans.

634

635 The dichotomy of continental vs oceanic tectonics may be viewed at least partially as a  
636 dichotomy of subaerial vs submarine tectonics.

637

638 Contrary to the long-held view of the ocean as incidental to plate tectonics, the ocean itself may  
639 well be a crucial element to the seafloor spreading process and potentially why Earth is the only  
640 known planet to exhibit plate tectonics.

641

642

### 643 **Acknowledgments**

644 I thank the SIU Board of Trustees for granting a sabbatical leave for work on this project.

645 Insightful comments and suggestions from Laurent Montesi and an anonymous reviewer greatly  
646 improved this manuscript. This work was partially supported by NSF grant EAR-1753637.

647

### 648 **Availability Statement**

649 No new data are presented in this manuscript. Software for calculating mass fluxes as isostatic  
650 response is housed at the SIU open software site: [https://opensiuc.lib.siu.edu/geol\\_comp/](https://opensiuc.lib.siu.edu/geol_comp/).

651

652 **References**

- 653
- 654 Arai, R., 2021. Characteristics of seismicity in the southern Okinawa Trough and their relation to  
655 back-arc rifting processes. *Earth Planets Space* 73, 10.1186/s40623-021-01491-4.
- 656 Arai, R., Kodaira, S., Yuka, K., Takahashi, T., Miura, S., Kaneda, Y., 2017. Crustal structure of  
657 the southern Okinawa Trough: Symmetrical rifting, submarine volcano, and potential mantle  
658 accretion in the continental back-arc basin. *J Geophys Res-Sol Ea* 122, 622-641,  
659 10.1002/2016jb013448.
- 660 Ashwal, L.D., Wiedenbeck, M., Torsvik, T.H., 2017. Archaean zircons in Miocene oceanic  
661 hotspot rocks establish ancient continental crust beneath Mauritius. *Nat Commun* 8,  
662 10.1038/ncomms14086.
- 663 Bastow, I.D., Keir, D., 2011. The protracted development of the continent-ocean transition in  
664 Afar. *Nat Geosci* 4, 248-250, 10.1038/Ngeo1095.
- 665 Becker, T.W., O'Connell, R.J., 2001. Predicting plate velocities with mantle circulation models.  
666 *Geochem Geophys Geosy* 2, Doi: 10.1029/2001gc000171.
- 667 Behn, M.D., Conrad, C.P., Silver, P.G., 2004. Detection of upper mantle flow associated with the  
668 African Superplume. *Earth and Planetary Science Letters* 224, 259-274,  
669 10.1016/j.epsl.2004.05.026.
- 670 Bennett, R.A., Davis, J.L., Normandeau, J.E., Wernicke, B.P., 2002. Space geodetic  
671 measurements of plate boundary deformation in the western U.S. cordillera, in: Stein, S.,  
672 Freymueller, J.T. (Eds.), *Plate Boundary Zones*. American Geophysical Union, Washinton,  
673 D.C., pp. 27-55.
- 674 Bennett, S.E.K., Oskin, M.E., Dorsey, R.J., Iriondo, A., Kunk, M.J., 2015. Stratigraphy and  
675 structural development of the southwest Isla Tiburon marine basin: Implications for latest  
676 Miocene tectonic opening and flooding of the northern Gulf of California. *Geosphere* 11,  
677 977-1007, 10.1130/Ges01153.1.
- 678 Bercovici, D., 1998. Generation of plate tectonics from lithosphere-mantle flow and void-volatile  
679 self-lubrication. *Earth and Planetary Science Letters* 154, 139-151, Doi 10.1016/S0012-  
680 821x(97)00182-9.
- 681 Bercovici, D., Ricard, Y., Richards, M.A., 2000. The relation between mantle dynamics and  
682 plate tectonics: A Primer, in: Richards, A., Gordon, R.G., van der Hilst, R.D. (Eds.), *The*  
683 *History and dynamics of global plate motions*. American Geophysical Union, Washington,  
684 D.C.
- 685 Bialas, R.W., Buck, W.R., 2009. How sediment promotes narrow rifting: Application to the Gulf  
686 of California. *Tectonics* 28, 10.1029/2008tc002394.
- 687 Bialas, R.W., Buck, W.R., Qin, R., 2010. How much magma is required to rift a continent? *Earth*  
688 *and Planetary Science Letters* 292, 68-78, 10.1016/j.epsl.2010.01.021.
- 689 Bilek, S.L., Lay, T., 2018. Subduction zone megathrust earthquakes. *Geosphere* 14, 1468-1500,  
690 10.1130/Ges01608.1.
- 691 Bonvalot, S., Balmino, G., Briais, A., Kuhn, M., Peyrefitte, A., Vales, N., Biancale, R., Gabalda,  
692 G., Requin, F., Sarrailh, M., 2012. *World Gravity Map*. Commission for the Geological  
693 *Map of the World*, Paris.

- 694 Bott, M.H.P., Waghorn, G.D., Whittaker, A., 1989. Plate Boundary Forces at Subduction Zones  
695 and Trench-Arc Compression. *Tectonophysics* 170, 1-15, Doi 10.1016/0040-  
696 1951(89)90099-1.
- 697 Brune, S., Kolawole, F., Olive, J.A., Stamps, D.S., Buck, W.R., Buitter, S.J.H., Furman, T.,  
698 Shillington, D.J., 2023. Geodynamics of continental rift initiation and evolution. *Nat Rev*  
699 *Earth Env*, 10.1038/s43017-023-00391-3.
- 700 Brune, S., Williams, S.E., Butterworth, N.P., Muller, R.D., 2016. Abrupt plate accelerations  
701 shape rifted continental margins. *Nature* 536, 201-+
- 702 Buck, W., 2007. Dynamic Processes in Extensional and Compressional Settings: The Dynamics  
703 of Continental Breakup and Extension. *Treatise Geophys.* 6, 335–376. doi: 10.1016. doi 10,  
704 B978-044452748
- 705 Cawood, P.A., Hawkesworth, C.J., Pisarevsky, S.A., Dhuime, B., Capitanio, F.A., Nebel, O.,  
706 2018. Geological archive of the onset of plate tectonics. *Philos T R Soc A* 376,  
707 10.1098/rsta.2017.0405.
- 708 Chauvet, F., Sapin, F., Geoffroy, L., Ringenbach, J.C., Ferry, J.N., 2021. Conjugate volcanic  
709 passive margins in the austral segment of the South Atlantic - Architecture and  
710 development. *Earth-Science Reviews* 212, 10.1016/j.earscirev.2020.103461.
- 711 Cloos, M., Shreve, R.L., 1996. Shear-zone thickness and the seismicity of Chilean- and  
712 Marianas-type subduction zones. *Geology* 24, 107-110, Doi 10.1130/0091-  
713 7613(1996)024<0107:Sztats>2.3.Co;2.
- 714 Cochran, J.R., Kurras, G.J., Edwards, M.H., Coakley, B.J., 2003. The Gakkel Ridge:  
715 Bathymetry, gravity anomalies, and crustal accretion at extremely slow spreading rates. *J*  
716 *Geophys Res-Sol Ea* 108, 10.1029/2002jb001830.
- 717 Collier, J.S., McDermott, C., Warner, G., Gyori, N., Schnabel, M., McDermott, K., Horn, B.W.,  
718 2017. New constraints on the age and style of continental breakup in the South Atlantic from  
719 magnetic anomaly data. *Earth and Planetary Science Letters* 477, 27-40,  
720 10.1016/j.epsl.2017.08.007.
- 721 Coltice, N., Gerault, M., Ulvrova, M., 2017. A mantle convection perspective on global  
722 tectonics. *Earth-Science Reviews* 165, 120-150, 10.1016/j.earscirev.2016.11.006.
- 723 Coltice, N., Husson, L., Faccenna, C., Arnould, M., 2019. What drives tectonic plates? *Sci Adv*  
724 5, 10.1126/sciadv.aax4295.
- 725 Conder, J.A., 2012. Non-Pratt component of oceanic isostasy. *Lithosphere* 4, 430-434
- 726 Conder, J.A., 2022a. Oceanic isostasy as a trigger for the rift-to-drift transition. *Geology* 50, 843-  
727 847, <https://doi.org/10.1130/G49914.1>.
- 728 Conder, J.A., 2022b. Oceanic isostasy as a trigger for the rift-to-drift transition: REPLY.  
729 *Geology* 50, e555, <https://doi.org/10.1130/G50661Y.1>.
- 730 Conder, J.A., D.W.Forsyth, E.M.Parmentier, 2002. Asthenospheric flow and asymmetry of the  
731 East Pacific Rise, MELT area. *Journal of Geophysical Research* 107, 2344,  
732 doi:2310.1029/2001JB000807
- 733 Conder, J.A., Forsyth, D.W., 2001. Seafloor spreading on the Southeast Indian Ridge over the  
734 last one million years: a test of the Capricorn plate hypothesis. *Earth and Planetary Science*  
735 *Letters* 188, 91-105, Doi 10.1016/S0012-821x(01)00326-0.

- 736 Conrad, C.P., Behn, M.D., Silver, P.G., 2007. Global mantle flow and the development of  
737 seismic anisotropy: Differences between the oceanic and continental upper mantle. *J*  
738 *Geophys Res-Sol Ea* 112, 10.1029/2006jb004608.
- 739 Conrad, C.P., Lithgow-Bertelloni, C., 2002. How mantle slabs drive plate tectonics. *Science* 298,  
740 207-209, DOI 10.1126/science.1074161.
- 741 Corti, G., 2009. Continental rift evolution: From rift initiation to incipient break-up in the Main  
742 Ethiopian Rift, East Africa. *Earth-Science Reviews* 96, 1-53,  
743 10.1016/j.earscirev.2009.06.005.
- 744 Corti, G., Agostini, A., Keir, D., Van Wijk, J., Bastow, I.D., Ranalli, G., 2015. Magma-induced  
745 axial subsidence during final-stage rifting: Implications for the development of seaward-  
746 dipping reflectors. *Geosphere* 11, 563-571, 10.1130/Ges01076.1.
- 747 Crameri, F., Conrad, C.P., Montesi, L., Lithgow-Bertelloni, C.R., 2019. The dynamic life of an  
748 oceanic plate. *Tectonophysics* 760, 107-135, 10.1016/j.tecto.2018.03.016.
- 749 Davis, J.K., Lavier, L.L., 2017. Influences on the development of volcanic and magma-poor  
750 morphologies during passive continental rifting. *Geosphere* 13, 1524-1540,  
751 10.1130/Ges01538.1.
- 752 DeMets, C., Gordon, R.G., Argus, D.F., 2010. Geologically current plate motions. *Geophysical*  
753 *Journal International* 181, 1-80, 10.1111/j.1365-246X.2009.04491.x.
- 754 DeMets, C., Merkouriev, S., 2019. High-resolution reconstructions of South America plate  
755 motion relative to Africa, Antarctica and North America: 34 Ma to present. *Geophysical*  
756 *Journal International* 217, 1821-1853, 10.1093/gji/ggz087.
- 757 Denk, T., Grimsson, F., Zetter, R., Simonarson, L.A., 2011. The Biogeographic History of  
758 Iceland - The North Atlantic Land Bridge Revisited. *Top Geobiol* 35, 647-668,  
759 10.1007/978-94-007-0372-8\_12.
- 760 Druet, M., Munoz-Martin, A., Granja-Bruna, J.L., Carbo-Gorosabel, A., Acosta, J., Llanes, P.,  
761 Ercilla, G., 2018. Crustal Structure and Continent-Ocean Boundary Along the Galicia  
762 Continental Margin (NW Iberia): Insights From Combined Gravity and Seismic  
763 Interpretation. *Tectonics* 37, 1576-1604, 10.1029/2017tc004903.
- 764 Dunn, R.A., Martinez, F., Conder, J.A., 2013. Crustal construction and magma chamber  
765 properties along the Eastern Lau Spreading Center. *Earth and Planetary Science Letters* 371,  
766 112-124, 10.1016/j.epsl.2013.04.008.
- 767 Dymkova, D., Gerya, T., 2013. Porous fluid flow enables oceanic subduction initiation on Earth.  
768 *Geophysical Research Letters* 40, 5671-5676, 10.1002/2013gl057798.
- 769 Einarsson, P., 2008. Plate boundaries, rifts and transforms in Iceland. *Jökull* 58, 35-58
- 770 Einarsson, P., Hjartardottir, A.R., Hreinsdottir, S., Imsland, P., 2020. The structure of  
771 seismogenic strike-slip faults in the eastern part of the Reykjanes Peninsula Oblique Rift,  
772 SW Iceland. *Journal of Volcanology and Geothermal Research* 391,  
773 10.1016/j.jvolgeores.2018.04.029.
- 774 Ellis, D., Stoker, M.S., 2014. The Faroe-Shetland Basin: a regional perspective from the  
775 Paleocene to the present day and its relationship to the opening of the North Atlantic Ocean.  
776 *Geol Soc Spec Publ* 397, 11-31, 10.1144/Sp397.1.
- 777 England, P., Jackson, J., 1989. Active Deformation of the Continents. *Annu Rev Earth Pl Sc* 17,  
778 197-226, DOI 10.1146/annurev.ea.17.050189.001213.

- 779 Forsyth, D., Uyeda, S., 1975. On the relative importance of the driving forces of plate motion.  
780 *Geophysical Journal International* 43, 163-200
- 781 Foulger, G.R., Dore, T., Emeleus, C.H., Franke, D., Geoffroy, L., Gernigon, L., Hey, R.,  
782 Holdsworth, R.E., Hole, M., Hoskuldsson, A., Julian, B., Kuszniir, N., Martinez, F.,  
783 McCaffrey, K.J.W., Natland, J.H., Peace, A.L., Petersen, K., Schiffer, C., Stephenson, R.,  
784 Stoker, M., 2020. The Iceland Microcontinent and a continental Greenland-Iceland-Faroe  
785 Ridge. *Earth-Science Reviews* 206, 10.1016/j.earscirev.2019.102926.
- 786 Fournier, M., Fabbri, O., Angelier, J., Cadet, J.P., 2001. Regional seismicity and on-land  
787 deformation in the Ryukyu arc: Implications for the kinematics of opening of the Okinawa  
788 Trough. *J Geophys Res-Sol Ea* 106, 13751-13768, Doi 10.1029/2001jb900010.
- 789 Fowler, C.M.R., Fowler, C.M.R., Fowler, M., 1990. *The solid earth: an introduction to global*  
790 *geophysics*. Cambridge University Press.
- 791 Franke, D., 2013. Rifting, lithosphere breakup and volcanism: Comparison of magma-poor and  
792 volcanic rifted margins. *Marine and Petroleum geology* 43, 63-87
- 793 Geoffroy, L., 2005. Volcanic passive margins. *Cr Geosci* 337, 1395-1408,  
794 10.1016/j.crte.2005.10.006.
- 795 GeoPRISMS, 2015. *GeoPRISMS Review - Rift Initiation and Evolution (RIE) initiative*.
- 796 Gerya, T.V., Stern, R.J., Baes, M., Sobolev, S.V., Whattam, S.A., 2015. Plate tectonics on the  
797 Earth triggered by plume-induced subduction initiation. *Nature* 527, 221-+,  
798 10.1038/nature15752.
- 799 Ghomsi, F.E.K., Tenzer, R., Njinju, E., Steffen, R., 2022. The crustal configuration of the West  
800 and Central African Rift System from gravity and seismic data analysis. *Geophysical*  
801 *Journal International* 230, 995-1012, 10.1093/gji/ggac089.
- 802 Ghosh, A., Holt, W.E., Wen, L.M., 2013. Predicting the lithospheric stress field and plate  
803 motions by joint modeling of lithosphere and mantle dynamics. *J Geophys Res-Sol Ea* 118,  
804 346-368, 10.1029/2012jb009516.
- 805 Goes, S., Agrusta, R., van Hunen, J., Garel, F., 2017. Subduction-transition zone interaction: A  
806 review. *Geosphere* 13, 644-664, 10.1130/Ges01476.1.
- 807 Gordon, R.G., 1998. The plate tectonic approximation: Plate nonrigidity, diffuse plate  
808 boundaries, and global plate reconstructions. *Annu Rev Earth Pl Sc* 26, 615-642, DOI  
809 10.1146/annurev.earth.26.1.615.
- 810 Gordon, R.G., 2023. Tectonic strain rates, diffuse oceanic plate boundaries, and the plate tectonic  
811 approximation, in: Duarte, J.C. (Ed.), *Dynamics of plate tectonics and mantle convection*.  
812 Elsevier, Cambridge, MA, pp. 83-103.
- 813 Gordon, R.G., Stein, S., 1992. Global Tectonics and Space Geodesy. *Science* 256, 333-342, DOI  
814 10.1126/science.256.5055.333.
- 815 Gouiza, M., Paton, D., 2017. Magma-poor vs. magma-rich continental rifting and breakup in the  
816 Labrador Sea, AGU Fall Meeting Abstracts, pp. T44A-05.
- 817 Grevemeyer, I., Ranero, C.R., Papenberg, C., Sallares, V., Bartolome, R., Prada, M., Batista, L.,  
818 Neres, M., 2022. The continent-to-ocean transition in the Iberia Abyssal Plain. *Geology* 50,  
819 615-619, 10.1130/G49753.1.

- 820 Ha, G., Montesi, L.G.J., Zhu, W.L., 2020. Melt Focusing Along Permeability Barriers at  
821 Subduction Zones and the Location of Volcanic Arcs. *Geochem Geophys Geosy* 21,  
822 10.1029/2020GC009253.
- 823 Harris, R.N., Conder, J.A., Heuret, A., 2014. The thermal structure of the subduction thrust  
824 within accretionary and erosive margins. *Tectonophysics* 633, 221-231,  
825 10.1016/j.tecto.2014.07.009.
- 826 Hasterok, D., Halpin, J.A., Collins, A.S., Hand, M., Kreemer, C., Gard, M.G., Glorie, S., 2022.  
827 New Maps of Global Geological Provinces and Tectonic Plates. *Earth-Science Reviews* 231,  
828 10.1016/j.earscirev.2022.104069.
- 829 Hayford, J.F., 1911. The relations of isostasy to Geodesy, Geophysics and Geology. *Science* 33,  
830 199-208
- 831 Heine, C., Zoethout, J., Müller, R.D., 2013. Kinematics of the South Atlantic rift. *Solid Earth* 4,  
832 215-253
- 833 Heuret, A., Lallemand, S., 2005. Plate motions, slab dynamics and back-arc deformation.  
834 *Physics of the Earth and Planetary Interiors* 149, 31-51, 10.1016/j.pepi.2004.08.022.
- 835 Holmes, A., 1931. Radioactivity and earth movements. *Trans. Geol. Soc. Glasgow* 18, 559-606
- 836 Hudson, M.R., Grauch, V.J.S., 2013. New Perspectives on Rio Grande Rift Basins: From  
837 Tectonics to Groundwater Introduction. *New Perspectives on Rio Grande Rift Basins: From*  
838 *Tectonics to Groundwater* 494, V-Xii, 10.1130/2013.2494(00).
- 839 Jackson, M.P.A., Cramez, C., Fonck, J.M., 2000. Role of subaerial volcanic rocks and mantle  
840 plumes in creation of South Atlantic margins: implications for salt tectonics and source  
841 rocks. *Marine and Petroleum Geology* 17, 477-498, Doi 10.1016/S0264-8172(00)00006-4.
- 842 Karner, G.D., Johnson, C.A., Figueredo, P., 2020. Tectonic significance of passive margin  
843 breakup magmatic packages. *GFZ Potsdam, Rift and rifted margins online seminar*.
- 844 Karson, J.A., 2017. The Iceland Plate Boundary Zone: Propagating Rifts, Migrating Transforms,  
845 and Rift-Parallel Strike-Slip Faults. *Geochem Geophys Geosy* 18, 4043-4054,  
846 10.1002/2017gc007045.
- 847 King, M.T., Welford, J.K., Peace, A.L., 2020. Investigating the role of the Galicia Bank on the  
848 formation of the North West Iberian margin using deformable plate tectonic models.  
849 *Tectonophysics* 789, 10.1016/j.tecto.2020.228537.
- 850 Kneller, E.A., Johnson, C.A., Karner, G.D., Einhorn, J., Queffelec, T.A., 2012. Inverse methods  
851 for modeling non-rigid plate kinematics: Application to mesozoic plate reconstructions of  
852 the Central Atlantic. *Comput Geosci-Uk* 49, 217-230, 10.1016/j.cageo.2012.06.019.
- 853 Kolzenburg, S., Kubanek, J., Dirscherl, M., Hamilton, C.W., Hauber, E., Scheidt, S.P., Munzer,  
854 U., 2022. Solid as a rock: Tectonic control of graben extension and dike propagation.  
855 *Geology* 50, 260-265, 10.1130/G49406.1.
- 856 Kumar, P., Mishra, A., Pitchika, V.K., Kumar, S., Dubey, K.M., Singh, D., Chaubey, A.K.,  
857 2019. Integrated geophysical appraisal of crustal structure and tectonic evolution of the  
858 Angria Bank, western continental India. *Marine Geophysical Researches* 40, 433-449,  
859 <https://doi.org/10.1007/s11001-019-09383-9>.
- 860 Lavier, L.L., Manatschal, G., 2006. A mechanism to thin the continental lithosphere at magma-  
861 poor margins. *Nature* 440, 324-328, 10.1038/nature04608.

- 862 Leat, P.T., Fretwell, P.T., Tate, A.J., Larter, R.D., Martin, T.J., Smellie, J.L., Jokat, W.,  
863 Bohrmann, G., 2016. Bathymetry and geological setting of the South Sandwich Islands  
864 volcanic arc. *Antarct Sci* 28, 293-303, 10.1017/S0954102016000043.
- 865 Lizarralde, D., Axen, G.J., Brown, H.E., Fletcher, J.M., González-Fernández, A., Harding, A.J.,  
866 Holbrook, W.S., Kent, G.M., Paramo, P., Sutherland, F., 2007. Variation in styles of rifting  
867 in the Gulf of California. *Nature* 448, 466-469
- 868 Macdonald, K.C., 1982. Mid-Ocean Ridges - Fine Scale Tectonic, Volcanic and Hydrothermal  
869 Processes within the Plate Boundary Zone. *Annu Rev Earth Pl Sc* 10, 155-190, DOI  
870 10.1146/annurev.ea.10.050182.001103.
- 871 Martin, P., van Hunen, J., Parman, S., Davidson, J., 2008. Why does plate tectonics occur only  
872 on Earth? *Physics Education* 43, 144-150, 10.1088/0031-9120/43/2/002.
- 873 Martin-Barajas, A., Gonzalez-Escobar, M., Fletcher, J.M., Pacheco, M., Oskin, M., Dorsey, R.,  
874 2013. Thick deltaic sedimentation and detachment faulting delay the onset of continental  
875 rupture in the Northern Gulf of California: Analysis of seismic reflection profiles. *Tectonics*  
876 32, 1294-1311, 10.1002/tect.20063.
- 877 Martinez, F., Okino, K., Ohara, Y., Reysenbach, A.L., Goffredi, S.K., 2007. Back-arc basins.  
878 *Oceanography* 20, 116-127
- 879 Martinez, F., Taylor, B., 2003. Controls on back-arc crustal accretion: insights from the Lau,  
880 Manus and Mariana basins. Geological Society, London, Special Publications 219, 19-54
- 881 Martinez, F., Taylor, B., 2006. Modes of crustal accretion in back-arc basins: Inferences from the  
882 Lau Basin. *Geophys Monogr Ser* 166, 5-+
- 883 Michaud, F., Royer, J.Y., Bourgois, J., Dymant, J., Calmus, T., Bandy, W., Sosson, M., Mortera-  
884 Gutierrez, C., Sichler, B., Rebolledo-Viera, M., Pontoise, B., 2006. Oceanic-ridge  
885 subduction vs. slab break off: Plate tectonic evolution along the Baja California Sur  
886 continental margin since 15 Ma. *Geology* 34, 13-16, 10.1130/G22050.1.
- 887 Molnar, P., 1988. Continental Tectonics in the Aftermath of Plate-Tectonics. *Nature* 335, 131-  
888 137, DOI 10.1038/335131a0.
- 889 Moulin, M., Aslanian, D., Unternehr, P., 2010. A new starting point for the South and Equatorial  
890 Atlantic Ocean. *Earth-Science Reviews* 98, 1-37
- 891 Mutter, J.C., Talwani, M., Stoffa, P.L., 1982. Origin of Seaward-Dipping Reflectors in Oceanic-  
892 Crust Off the Norwegian Margin by Subaerial Sea-Floor Spreading. *Geology* 10, 353-357,  
893 Doi 10.1130/0091-7613(1982)10<353:Oosrio>2.0.Co;2.
- 894 Naliboff, J.B., Conrad, C.P., Lithgow-Bertelloni, C., 2009. Modification of the lithospheric stress  
895 field by lateral variations in plate-mantle coupling. *Geophysical Research Letters* 36,  
896 10.1029/2009gl040484.
- 897 Nance, R.D., Murphy, J.B., 2013. Origins of the supercontinent cycle. *Geosci Front* 4, 439-448,  
898 10.1016/j.gsf.2012.12.007.
- 899 Nauret, F., Famin, V., Vlastelic, I., Gannoun, A., 2019. A trace of recycled continental crust in  
900 the Reunion hotspot. *Chem Geol* 524, 67-76, 10.1016/j.chemgeo.2019.06.009.
- 901 Nishimura, S., Hashimoto, M., Ando, M., 2004. A rigid block rotation model for the GPS  
902 derived velocity field along the Ryukyu arc. *Physics of the Earth and Planetary Interiors*  
903 142, 185-203, 10.1016/j.pepi.2003.12.014.

- 904 Nishizawa, A., Kaneda, K., Oikawa, M., Horiuchi, D., Fujioka, Y., Okada, C., 2019. Seismic  
905 structure of rifting in the Okinawa Trough, an active backarc basin of the Ryukyu (Nansei-  
906 Shoto) island arc-trench system. *Earth Planets Space* 71, 10.1186/s40623-019-0998-6.
- 907 O'Neill, C., Marchi, S., Zhang, S., Bottke, A., 2017. Impact-driven subduction on the Hadean  
908 Earth. *Nat Geosci* 10, 793-+, 10.1038/Ngeo3029.
- 909 Ojakangas, R.W., Morey, G.B., Green, J.C., 2001. The Mesoproterozoic Midcontinent Rift  
910 System, Lake Superior Region, USA. *Sediment Geol* 141, 421-442, Doi 10.1016/S0037-  
911 0738(01)00085-9.
- 912 Parsons, B., Sclater, J.G., 1977. Analysis of Variation of Ocean-Floor Bathymetry and Heat-  
913 Flow with Age. *Journal of Geophysical Research* 82, 803-827, DOI  
914 10.1029/JB082i005p00803.
- 915 Perez-Gussinye, M., Collier, J.S., Armitage, J.J., Hopper, J.R., Sun, Z., Ranero, C.R., 2023.  
916 Towards a process-based understanding of rifted continental margins. *Nat Rev Earth Env* 4,  
917 166-184, 10.1038/s43017-022-00380-y.
- 918 Peron-Pinvidic, G., Manatschal, G., Alves, T., Andersen, T., Andres-Martinez, M., Autin, J.,  
919 Ball, P., Brune, S., Buitter, S., Cadenas, P., Cresswell, D., Epin, M.E., Gomez-Romeu, J.,  
920 Gouiza, M., Harkin, C., Heine, C., Hopper, J., Jackson, C., Jolivet, L., Katz, R., Lescoutre,  
921 R., Lymer, G., Magee, C., Masini, M., Miro, J., Molnar, N., Mouthereau, F., Muntener, O.,  
922 Naliboff, J., Norcliffe, J., Osmundsen, P.T., Diaz, L.P., Phillips, T.P., Ramos, A., Ranero,  
923 C., Reston, T., Ribes, C., Rooney, T., Rowan, M., Snidero, M., Tugend, J., Wang, L.J.,  
924 Zwaan, F., Partici, I.R.W., 2019. Rifted Margins: State of the Art and Future Challenges.  
925 *Front Earth Sc-Switz* 7
- 926 Phipps Morgan, J., Parmentier, E.M., Lin, J., 1987. Mechanisms for the Origin of Midocean  
927 Ridge Axial Topography - Implications for the Thermal and Mechanical Structure of  
928 Accreting Plate Boundaries. *J Geophys Res-Solid* 92, 12823-12836, DOI  
929 10.1029/JB092iB12p12823.
- 930 Polteau, S., Mazzini, A., Hansen, G., Planke, S., Jerram, D.A., Millett, J., Abdelmalak, M.M.,  
931 Blischke, A., Myklebust, R., 2019. The pre-breakup stratigraphy and petroleum system of  
932 the Southern Jan Mayen Ridge revealed by seafloor sampling. *Tectonophysics* 760, 152-  
933 164, 10.1016/j.tecto.2018.04.016.
- 934 Regenauer-Lieb, K., Yuen, D.A., Branlund, J., 2001. The initiation of subduction: Criticality by  
935 addition of water? *Science* 294, 578-580, DOI 10.1126/science.1063891.
- 936 Ross, J.E., Kidwell, S.M., Dettman, D.L., Bright, J., Dorsey, R.J., and Jefferson, G.T., 2020.  
937 Evidence of Pleistocene Marine Incursions into the Salton Basin, in: Miller, D.M. (Ed.),  
938 *Changing Facies. 2020 Desert Research Symposium.*
- 939 Royer, J.Y., Gordon, R.G., 1997. The motion and boundary between the Capricorn and  
940 Australian plates. *Science* 277, 1268-1274, DOI 10.1126/science.277.5330.1268.
- 941 Saemundsson, K., Sigurgeirsson, M.A., Fridleifsson, G.O., 2020. Geology and structure of the  
942 Reykjanes volcanic system, Iceland. *Journal of Volcanology and Geothermal Research* 391,  
943 10.1016/j.jvolgeores.2018.11.022.
- 944 Sandwell, D.T., 2001. Plate tectonics: A Martian view, in: Oreskes, N. (Ed.), *Plate Tectonics: An*  
945 *insider's history of the modern theory of the Earth.* Westview Press, Cambridge, MA.

- 946 Sandwell, D.T., Muller, R.D., Smith, W.H.F., Garcia, E., Francis, R., 2014. New global marine  
947 gravity model from CryoSat-2 and Jason-1 reveals buried tectonic structure. *Science* 346,  
948 65-67, 10.1126/science.1258213.
- 949 Santos, R.V., Ganade, C.E., Lacasse, C.M., Costa, I.S.L., Pessanha, I., Frazao, E.P., Dantas,  
950 E.L., Cavalcante, J.A., 2019. Dating Gondwanan continental crust at the Rio Grande Rise,  
951 South Atlantic. *Terra Nova* 31, 424-429, 10.1111/ter.12405.
- 952 Sapin, F., Ringenbach, J.C., Clerc, C., 2021. Rifted margins classification and forcing  
953 parameters. *Sci Rep-Uk* 11
- 954 Scotchman, I.C., Gilchrist, G., Kusznir, N.J., Roberts, A.M., Fletcher, R., 2010. The breakup of  
955 the South Atlantic Ocean: formation of failed spreading axes and blocks of thinned  
956 continental crust in the Santos Basin, Brazil and its consequences for petroleum system  
957 development. *Petrol Geol Conf P*, 855-866, 10.1144/0070855.
- 958 Sdrolias, M., Muller, R.D., 2006. Controls on back-arc basin formation. *Geochem Geophys*  
959 *Geosy* 7, 10.1029/2005gc001090.
- 960 Shillington, D.J., Scott, C.L., Minshull, T.A., Edwards, R.A., Brown, P.J., White, N., 2009.  
961 Abrupt transition from magma-starved to magma-rich rifting in the eastern Black Sea.  
962 *Geology* 37, 7-10
- 963 Sigmundsson, F., Einarsson, P., Hjartardóttir, Á.R., Drouin, V., Jónsdóttir, K., Árnadóttir, T.,  
964 Geirsson, H., Hreinsdóttir, S., Li, S., Ófeigsson, B.G., 2020. Geodynamics of Iceland and  
965 the signatures of plate spreading. *Journal of Volcanology and Geothermal Research* 391,  
966 106436
- 967 Small, C., Buck, W.R., Delaney, P.T., Karson, J.A., Lagabrielle, Y., 1998. Global systematics of  
968 mid-ocean ridge morphology. American Geophysical Union, Washington, DC, pp. 1-25.
- 969 Stamps, D.S., Kreemer, C., Fernandes, R., Rajaonarison, T.A., Rambolamanana, G., 2021.  
970 Redefining East African Rift System kinematics. *Geology* 49, 150-155, 10.1130/G47985.1.
- 971 Stein, S., Sella, G.F., 2002. Plate boundary zones: Concept and approaches, in: Stein, S.,  
972 Freymueller, J.T. (Eds.), *Plate Boundary Zones*. American Geophysical union, Washington,  
973 D.C.
- 974 Stein, S., Stein, C.A., Elling, R., Kley, J., Keller, G.R., Wyssession, M., Rooney, T., Frederiksen,  
975 A., Moucha, R., 2018. Insights from North America's failed Midcontinent Rift into the  
976 evolution of continental rifts and passive continental margins. *Tectonophysics* 744, 403-421
- 977 Taylor, B., Goodliffe, A., Martinez, F., Hey, R., 1995. Continental rifting and initial sea-floor  
978 spreading in the Woodlark Basin. *Nature* 374, 534-537
- 979 Taylor, B., Zellmer, K., Martinez, F., Goodliffe, A.M., 1996. Sea-floor spreading in the Lau  
980 back-arc basin. *Earth and Planetary Science Letters* 144, 35-40
- 981 Thatcher, W., 1995. Microplate Versus Continuum Descriptions of Active Tectonic  
982 Deformation. *J Geophys Res-Sol Ea* 100, 3885-3894, Doi 10.1029/94jb03064.
- 983 Tugend, J., Gillard, M., Manatschal, G., Nirrengarten, M., Harkin, C., Epin, M.-E., Sauter, D.,  
984 Autin, J., Kusznir, N., Mcdermott, K., 2020. Reappraisal of the magma-rich versus magma-  
985 poor rifted margin archetypes. Geological Society, London, Special Publications 476, 23-47
- 986 Turcotte, D.L., Schubert, G., 2002. *Geodynamics*, 2nd ed. Cambridge University Press,  
987 Cambridge ; New York.

- 988 Umhoefer, P.J., 2011. Why did the southern Gulf of California rupture so rapidly?—Oblique  
989 divergence across hot, weak lithosphere along a tectonically active margin. *GSA today* 21,  
990 4-10
- 991 Umhoefer, P.J., Darin, M.H., Bennett, S.E., Skinner, L.A., Dorsey, R.J., Oskin, M.E., 2018.  
992 Breaching of strike-slip faults and successive flooding of pull-apart basins to form the Gulf  
993 of California seaway from ca. 8–6 Ma. *Geology* 46, 695-698
- 994 Umhoefer, P.J., Plattner, C., Malservisi, R., 2020. Quantifying rates of "rifting while drifting" in  
995 the southern Gulf of California: The role of the southern Baja California microplate and its  
996 eastern boundary zone. *Lithosphere* 12, 122-132, 10.1130/L1132.1.
- 997 Unternehr, P., Péron-Pinvidic, G., Manatschal, G., Sutra, E., 2010. Hyper-extended crust in the  
998 South Atlantic: in search of a model. *Petroleum Geoscience* 16, 207-215
- 999 Uyeda, S., 1987. Chilean Vs. Mariana Type Subduction Zones With Remarks on Arc Volcanism  
1000 and Collision Tectonics, in: Monger, J.W.H., Francheteau, J. (Eds.), *Circum-Pacific*  
1001 *Orogenic Belts and Evolution of the Pacific Ocean Basin*. American Geophysical Union, pp.  
1002 1-7.
- 1003 van der Lee, S., Regenauer-Lieb, K., Yuen, D.A., 2008. The role of water in connecting past and  
1004 future episodes of subduction. *Earth and Planetary Science Letters* 273, 15-27,  
1005 10.1016/j.epsl.2008.04.041.
- 1006 van Wijk, J., Axen, G., Abera, R., 2017. Initiation, evolution and extinction of pull-apart basins:  
1007 Implications for opening of the Gulf of California. *Tectonophysics* 719, 37-50,  
1008 10.1016/j.tecto.2017.04.019.
- 1009 van Wijk, J.W., Heyman, S.P., Axen, G.J., Persaud, P., 2019. Nature of the crust in the northern  
1010 Gulf of California and Salton Trough. *Geosphere* 15, 1598-1616, 10.1130/Ges02082.1.
- 1011 Von Herzen, R., Ruppel, C., Molnar, P., Nettles, M., Nagihara, S., Ekstrom, G., 2001. A  
1012 constraint on the shear stress at the Pacific-Australian plate boundary from heat flow and  
1013 seismicity at the Kermadec forearc. *J Geophys Res-Sol Ea* 106, 6817-6833, Doi  
1014 10.1029/2000jb900469.
- 1015 Wallace, L.M., McCaffrey, R., Beavan, J., Ellis, S., 2005. Rapid microplate rotations and  
1016 backarc rifting at the transition between collision and subduction. *Geology* 33, 857-860,  
1017 10.1130/G21834.1.
- 1018 Wang, M., Shen, Z.K., 2020. Present-Day Crustal Deformation of Continental China Derived  
1019 From GPS and Its Tectonic Implications. *J Geophys Res-Sol Ea* 125,  
1020 10.1029/2019JB018774.
- 1021 Wang, P., Huang, C.-Y., Lin, J., Jian, Z., Sun, Z., Zhao, M., 2019. The South China Sea is not a  
1022 mini-Atlantic: plate-edge rifting vs intra-plate rifting. *National Science Review* 6, 902-913
- 1023 Weeraratne, D., Manga, M., 1998. Transitions in the style of mantle convection at high Rayleigh  
1024 numbers. *Earth and Planetary Science Letters* 160, 563-568, Doi 10.1016/S0012-  
1025 821x(98)00111-3.
- 1026 Wiens, D.A., Demets, C., Gordon, R.G., Stein, S., Argus, D., Engeln, J.F., Lundgren, P., Quible,  
1027 D., Stein, C., Weinstein, S., Woods, D.F., 1985. A Diffuse Plate Boundary Model for  
1028 Indian-Ocean Tectonics. *Geophysical Research Letters* 12, 429-432, DOI  
1029 10.1029/GL012i007p00429.

- 1030 Worthington, L.L., Shuck, B.D., Becel, A., Eilon, Z.C., Lynner, C., 2021. Breaking up is hard to  
1031 do, especially for continents. *Eos* 102, <https://doi.org/10.1029/2021EO155889>.
- 1032 Zatman, S., Richards, M., A., 2002. On the evolution of motion across diffuse plate boundaries,  
1033 in: Stein, S., Freymueller, J.T. (Eds.), *Plate Boundary Zones*. American Geophysical Union,  
1034 Washington, D.C.
- 1035
- 1036

1037 **Figure captions.**

1038

1039 **Figure 1.** Figure from Hayford (1911) showing isostatic response of continual mass exchange at  
1040 the surface being balanced by a continual counter mass flux at depth. The ‘undertow’ mass flux  
1041 will induce stresses on the crust above, in this case resulting in compression in the crust near the  
1042 base of the mountain belt.

1043

1044 **Figure 2.** Asthenosphere isostatic response to surface mass exchange that occurs with  
1045 differential thermal subsidence at the seafloor. Cartoon is in a plate-fixed reference frame. Faster  
1046 subsidence regions (younger ages) gain mass more rapidly as water deepens than regions with  
1047 slower subsidence (older ages), inducing a counter mass flux that leads the plate in the plate  
1048 spreading direction. In this plate-fixed reference frame, plate growth is to the left.

1049

1050 **Figure 3.** Subaerial and submarine square root of age (a) and mass gain (b) curves (after Conder,  
1051 2012).  $\gamma$  corresponds to both the difference in the two curves and the height of asthenosphere  
1052 column equivalent to the mass of the overlying ocean.

1053

1054 **Figure 4.** Calculations for 1D across-axis isostatic response of differential thermal subsidence at  
1055 the seafloor. Top panel (a) shows seafloor thermal age to either side of a constant velocity,  
1056 symmetrically spreading ridge. Second panel (b) shows mass gain that comes with subsidence  
1057 and a deepening ocean. Dashed line is the mean gain line. To maintain gravitational equilibrium,  
1058 seafloor with ocean mass gains above the line must transfer asthenosphere mass to seafloor with  
1059 ocean mass gains below the line which have relative mass deficits. Third panel (c) shows the

1060 resulting asthenosphere mass flux to maintain equilibrium (left axis) and associated basal  
1061 tractions (right axis). Positive fluxes and tractions are directed to the right; Negative fluxes and  
1062 tractions are directed to the left. Equilibrium (zero) line is dashed. Directions of flow also  
1063 denoted by arrows. Bottom panel (d) shows the integrated outward push force at the seafloor as a  
1064 function of location. Positive values promote extension, negative values promote compression.  
1065 The push force peaks and tends to localize extension at the axis.

1066

1067 **Figure 5.** Example of two axes of extension. (a) shows thermal age across the system, with two  
1068 locations having zero age. (b) shows the isostatic mass flux response across the system after  
1069 submergence (left axis) and associated basal tractions (right axis). Dashed line is equilibrium. (c)  
1070 shows the outward mantle tractions associated with extension. When submergence occurs, the  
1071 isostatic response likely has preference for one of the axes to extend and reinforces localization  
1072 at the expense of the other.

1073

1074 **Figure 6.** Examples of random thermal structure of a rift and isostatic response after  
1075 submergence. (a) shows (randomly distributed) thermal ages across the system. (b) shows the  
1076 isostatic mass flux response across the system after submergence. (c) shows the mantle tractions  
1077 associated with extension. When submergence occurs, the isostatic response will likely result in  
1078 a preferred locus of extension that will reinforce itself with continued extension.

1079

1080 **Figure 7.** Morphology of the midocean ridge system across the Icelandic platform and coastline.  
1081 Ridge morphology changes are greatest across the Reykjanes Peninsula as opposed to across the  
1082 off-platform/on-platform transition. ‘RR’ stands for Reykjanes Ridge. ‘WRZ’, ‘ERZ’, and

1083 ‘NRZ’ stand for Western Rift Zone, Eastern Rift Zone, and Northern Rift Zone, respectively  
1084 (following *Karson* [2017]). Colors denote depth/elevation. Figure made in GeoMapApp  
1085 (*geomapapp.org*).

1086

1087 **Figure 8.** Isostatic gravity anomaly of Iceland and surrounding region (Bonvalot et al., 2012).  
1088 The isostatic anomaly being the difference from expected if the system were in Airy isostatic  
1089 equilibrium Thin black line denotes coastline. The edge of the platform where intersected by the  
1090 spreading system is also marked. Labels are same as in figure 6. ‘KR’ stands for Kolbeinsey  
1091 Ridge. Figure made in GeoMapApp (*geomapapp.org*).

1092

1093 **Figure 9.** Seismicity and slip vectors for extensional earthquakes on and around Iceland. Blue  
1094 circles are earthquakes of magnitude  $>4.5$  1960-2022. Thick black line denotes coastlines.  
1095 Medium thick black line is 400 m contour outlining the Iceland platform and thinner black lines  
1096 show deeper 200 m contour intervals. Black arrows show predicted slip direction based on  
1097 MORVEL Euler pole (DeMets et al., 2010). Green, cyan, magenta, and red lines show slip  
1098 directions for extensional earthquakes from 1990-2023 in the CMT catalog (*globalcmt.org*).  
1099 Extensional events are absent on the Reykjanes Peninsula as it is dominated by strike-slip  
1100 bookshelf faulting. Colors show deviations from predicted directions: Green within  $15^\circ$ , Cyan  
1101 within  $30^\circ$ , Magenta within  $45^\circ$ , and Red greater than  $45^\circ$  from predicted.

1102

1103 **Figure 10.** 1D calculations of mantle tractions for a representative oceanic region with a  
1104 subaerial portion (gray region) where the thermal age is youngest. Half-spreading rate is set to 10  
1105 km/Myr. Top panel (a) shows mass adjustments arising from subsidence with an overlying

1106 ocean. The subaerial region gains zero mass with subsidence. Dashed line is line of equilibration.  
1107 Middle panels (b&c) show the corresponding mass exchange (left axis) and associated basal  
1108 tractions (right axis) assuming that either the subaerial region participates in the mass exchange  
1109 (b) or does not participate (c). Bottom panels (d&e) show corresponding associated outward push  
1110 from induced mantle traction in b&c respectively. If the subaerial region fully participates in  
1111 isostatic equilibration, preferred localization is just outside the edges of the island (d); If  
1112 participation is limited, preferred localization is on the island itself but no preference beyond that  
1113 (e).

1114

1115 **Figure 11.** Gulf of California topography (a) and free air gravity anomaly (Sandwell v30) (b).  
1116 Plate boundary marked in red (extension) and black (transform). Boundary follows (Umhoefer et  
1117 al., 2020) and (Martin-Barajas et al., 2013). EPR = East Pacific Rise. The exact boundary is more  
1118 speculative in the northern gulf. The area of low free air gravity seen along the Gulf (thick  
1119 orange line; roughly the 0 mGal contour) extends to and terminates at the Salton trough in the  
1120 north indicating the extent of the region where isostatic accommodation process is correlated.  
1121 The continental-oceanic crustal boundary is clear in the gravity across the gulf, but is subdued  
1122 along the gulf. Figure made in GeoMapApp ([geomapapp.org](http://geomapapp.org)).

1123

1124 **Figure 12.** South Atlantic plate reconstructions at 120 and 115 Ma from Heine et al. (2013).  
1125 Purple arrows show seafloor spreading propagation direction. A continuous northward  
1126 progression stalled at ~120 Ma at the Sao Paulo High (SPH). Spreading pick up a few million  
1127 years later to the north, again propagating northward, but also southward back to the SPH. The  
1128 connection between the two is made on the African side of the high. The orange star denotes the

1129 location of the extinct Abimael propagator (Sandwell et al., 2014) that propagated northward on  
1130 the South American side of the SPH before succumbing to spreading on the other side of the  
1131 high.

1132

1133 **Figure 13.** Bathymetry of the Marianas (a) and Okinawa Trough (b) backarc spreading systems.  
1134 Colorbar is the same for both. The Marianas is a typical ocean-ocean backarc system. The mostly  
1135 submerged arc system and remnant arc rafted off with spreading can be clearly observed. The  
1136 Okinawa trough is a ocean-continent backarc system where extension is occurring much like that  
1137 seen in ocean-ocean systems. Extension has thinned the continental crust to where distinct rift  
1138 axes can be observed in the southern system. Figures made in GeoMapApp ([geomapapp.org](http://geomapapp.org)).

1139

1140 **Figure 14.** Diffuse plate boundaries from Stein and Sella (2002). Stippling indicates diffuse  
1141 tectonic boundaries as well as their overall character. Broad seismicity, topography and faulting  
1142 tends to characterize subaerial plate boundaries. Virtually all subaerial boundaries can be  
1143 classified as diffuse. A smaller percentage of submarine boundaries can be classified as diffuse.  
1144 Submarine diffuse plate boundaries tend to be more subtle than subaerial diffuse boundaries and  
1145 identifiable by plate closure and/or a moderate number of earthquakes. The mid-ocean ridge  
1146 system tends to be narrow and non-diffuse.

1147

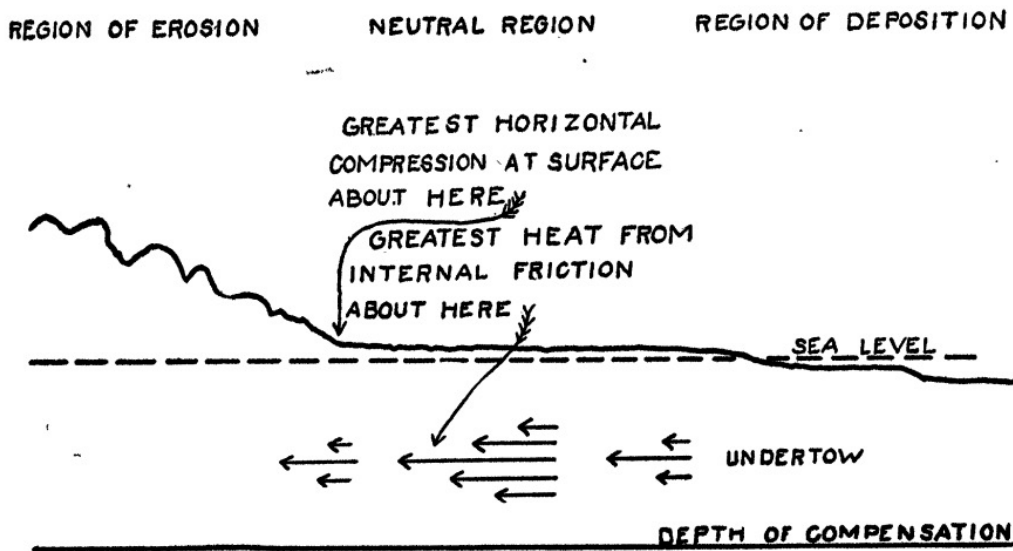


Figure 1

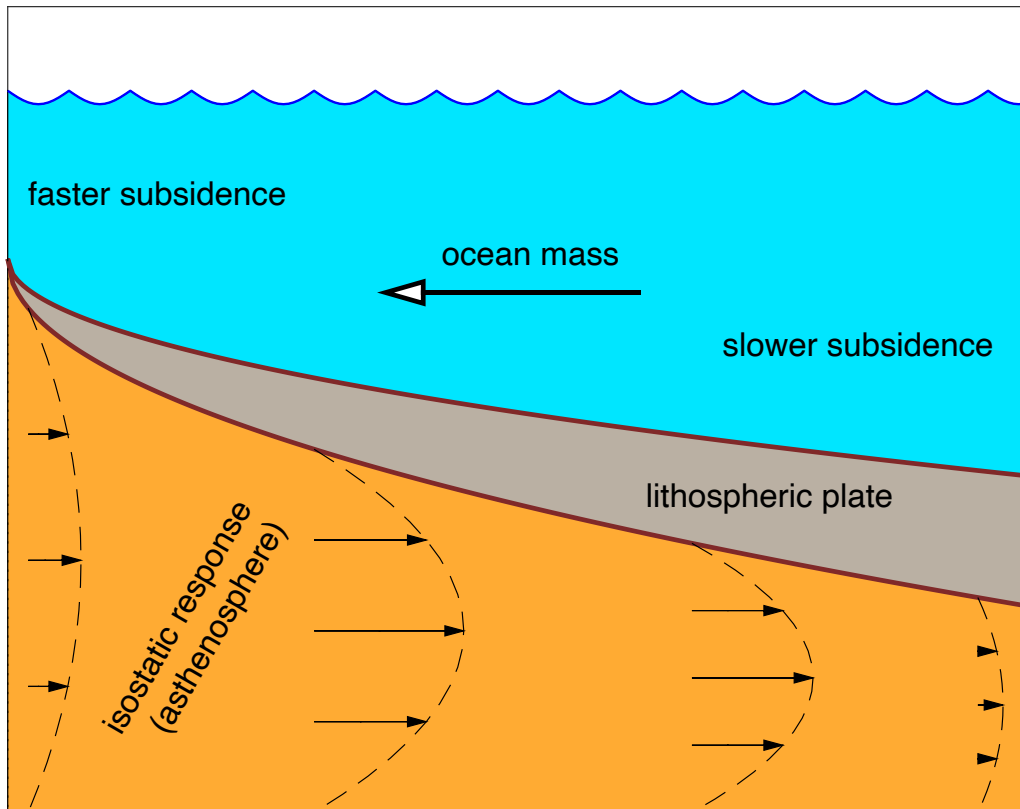


Figure 2

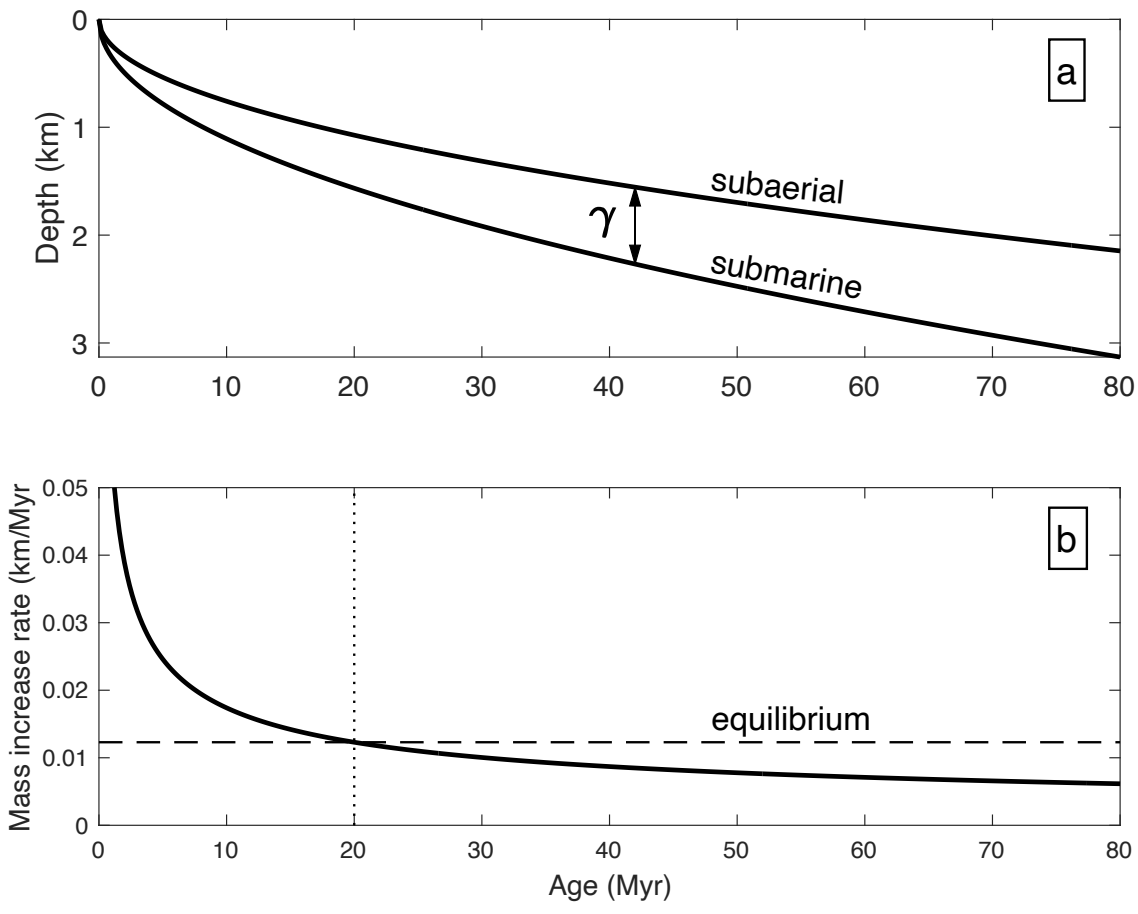


Figure 3

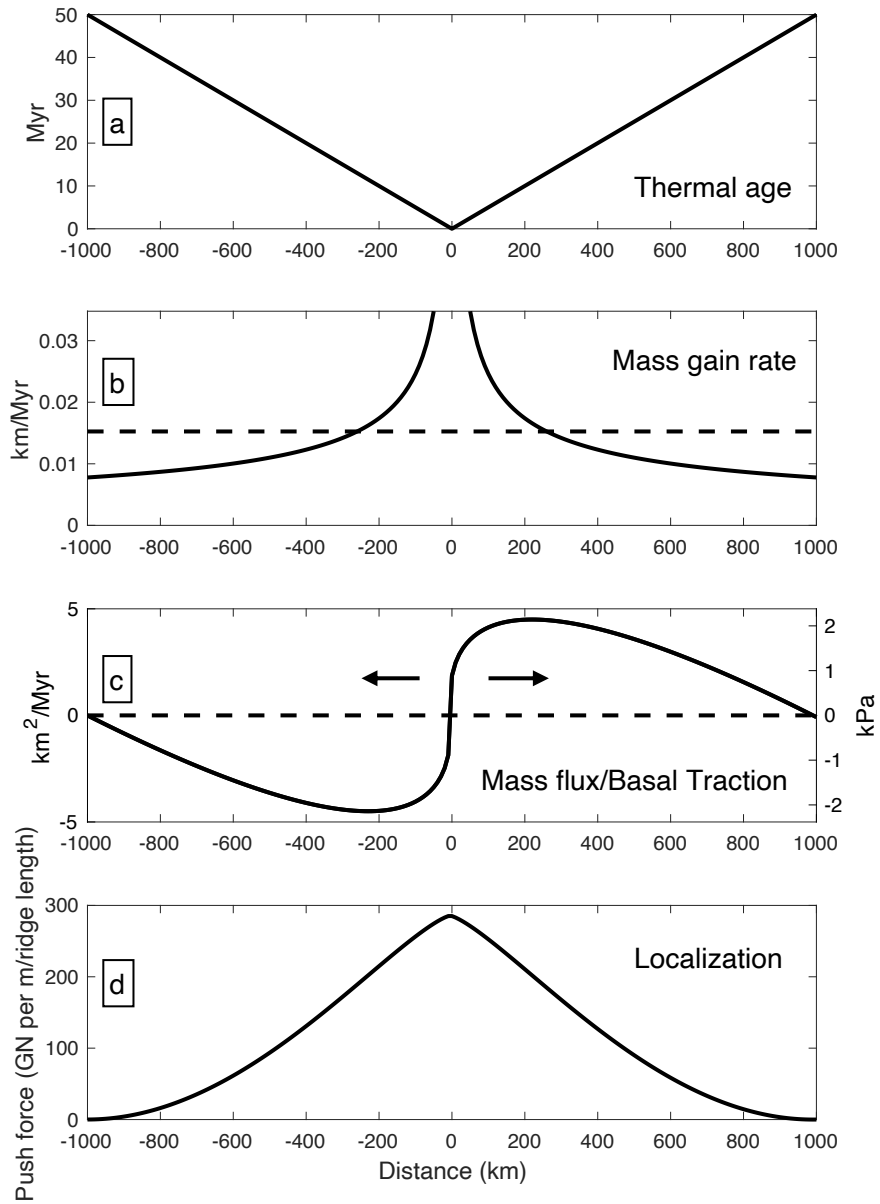


Figure 4

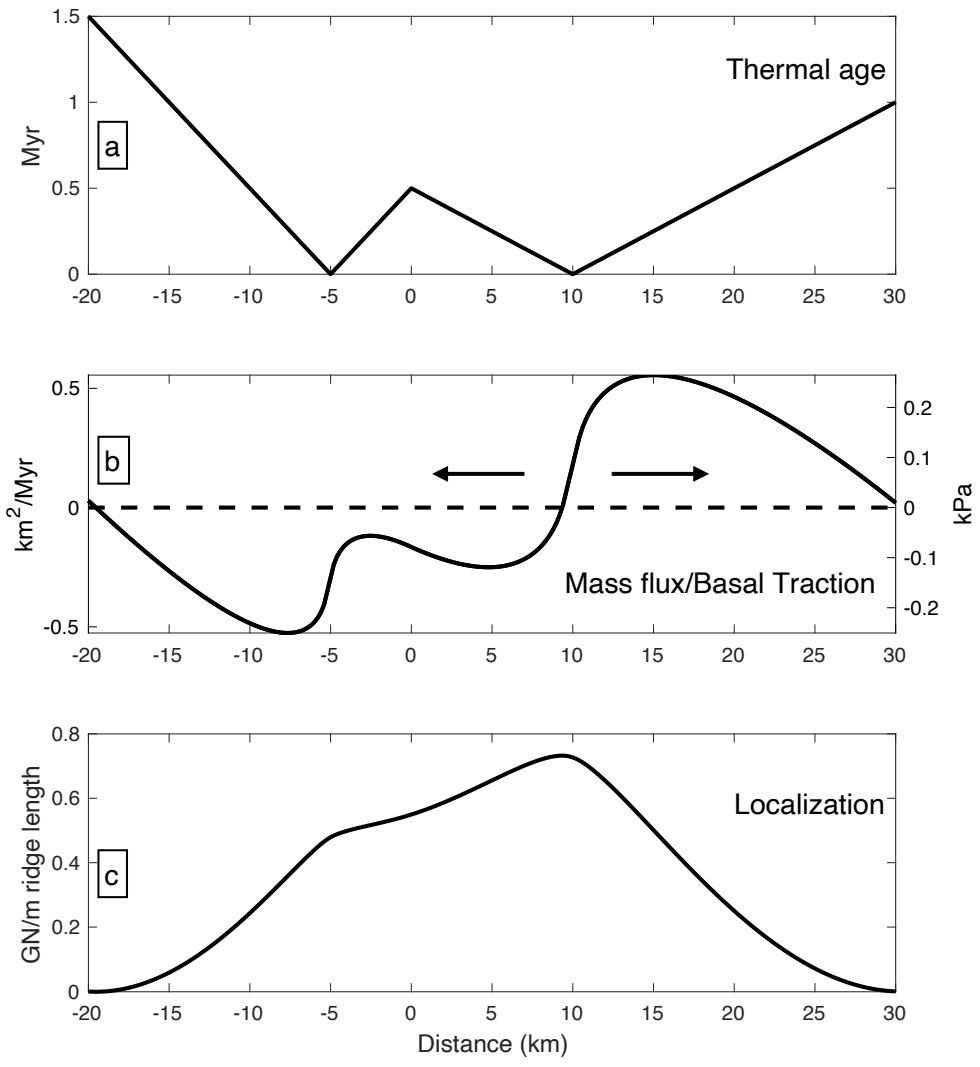


Figure 5

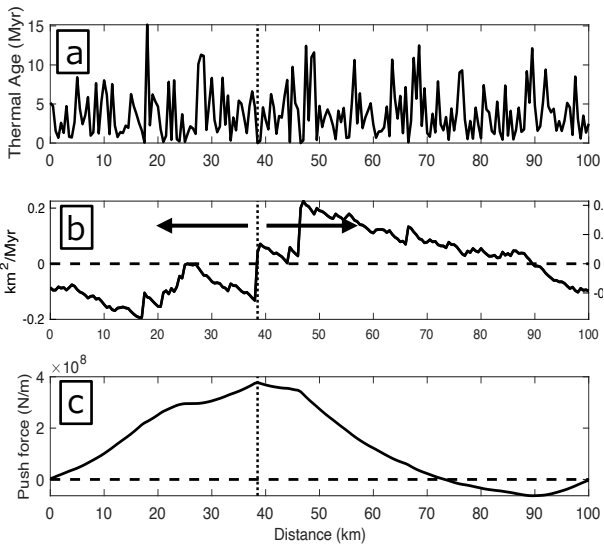


Figure 6

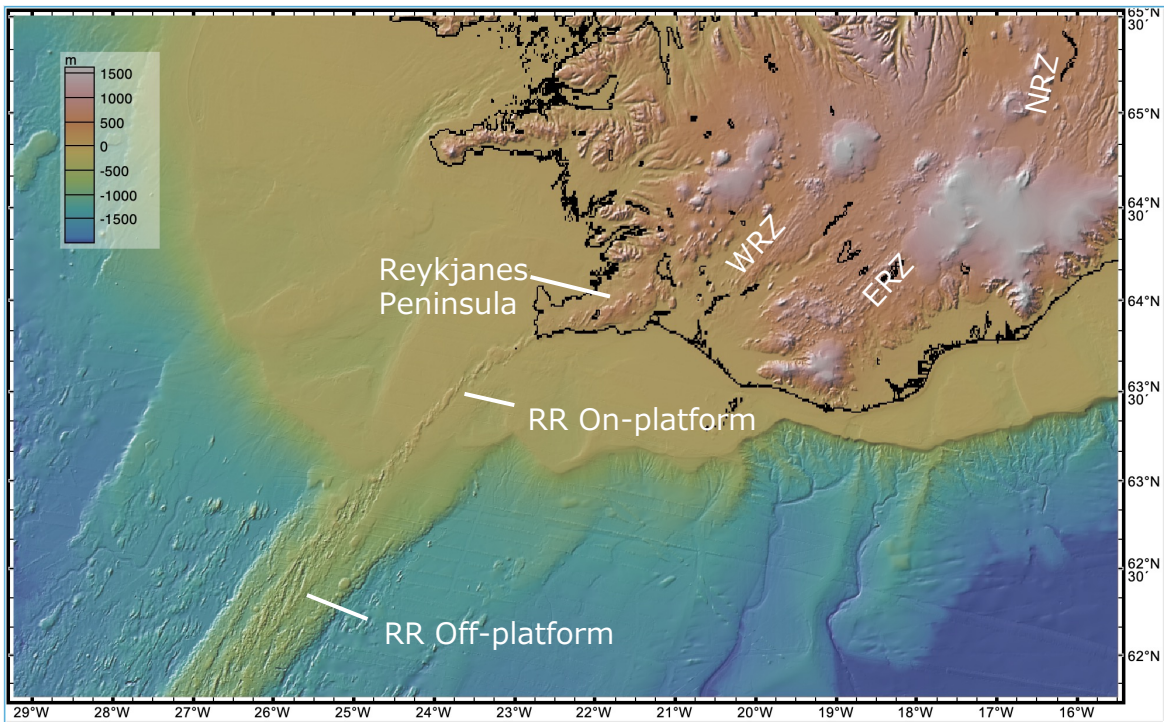


Figure 7

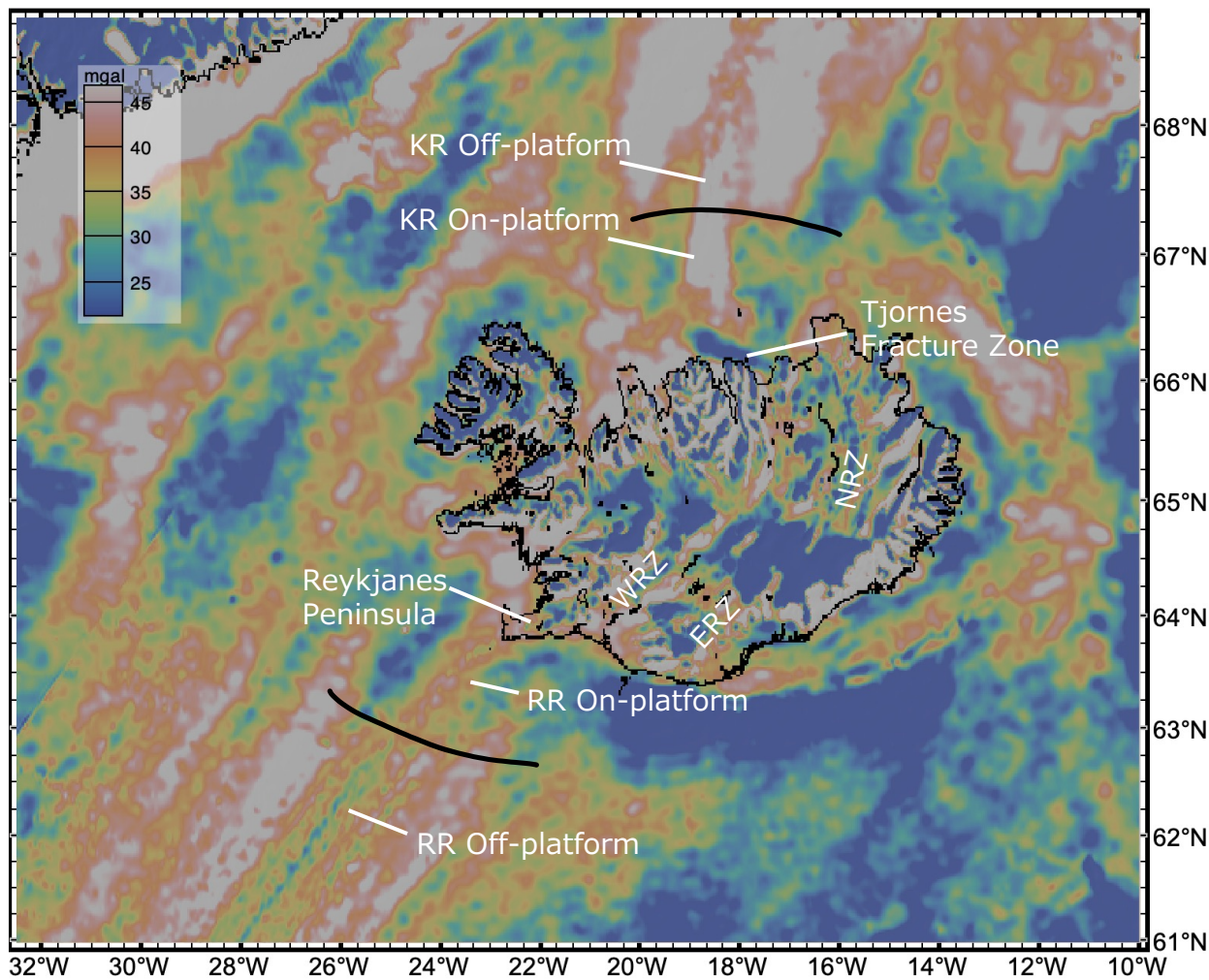


Figure 8

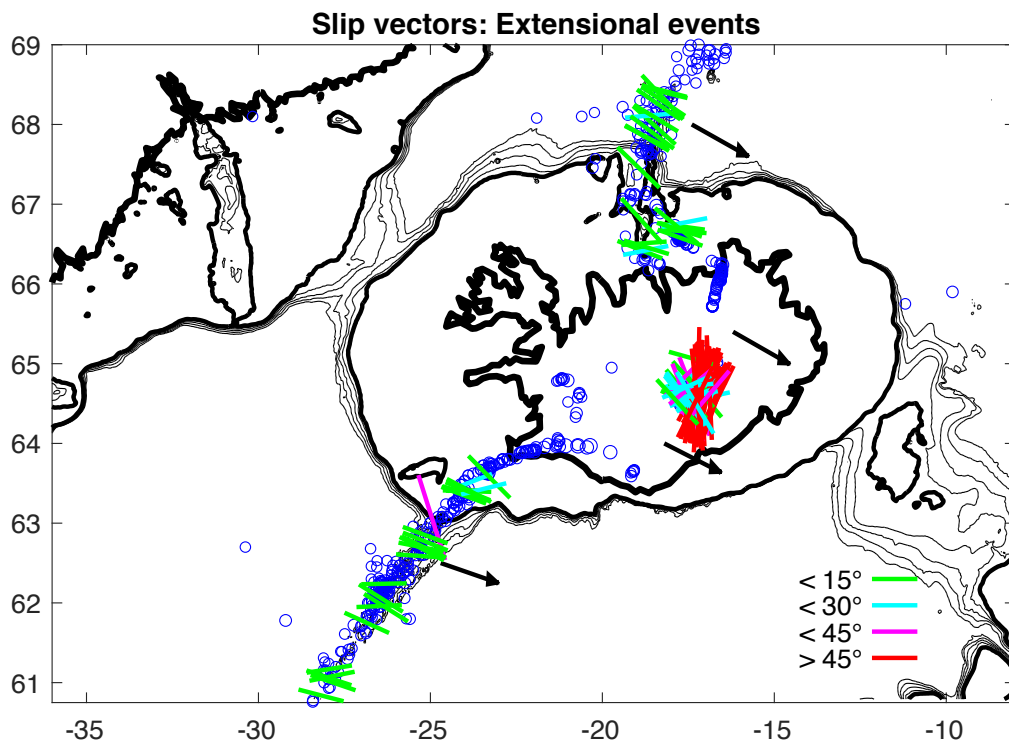


Figure 9

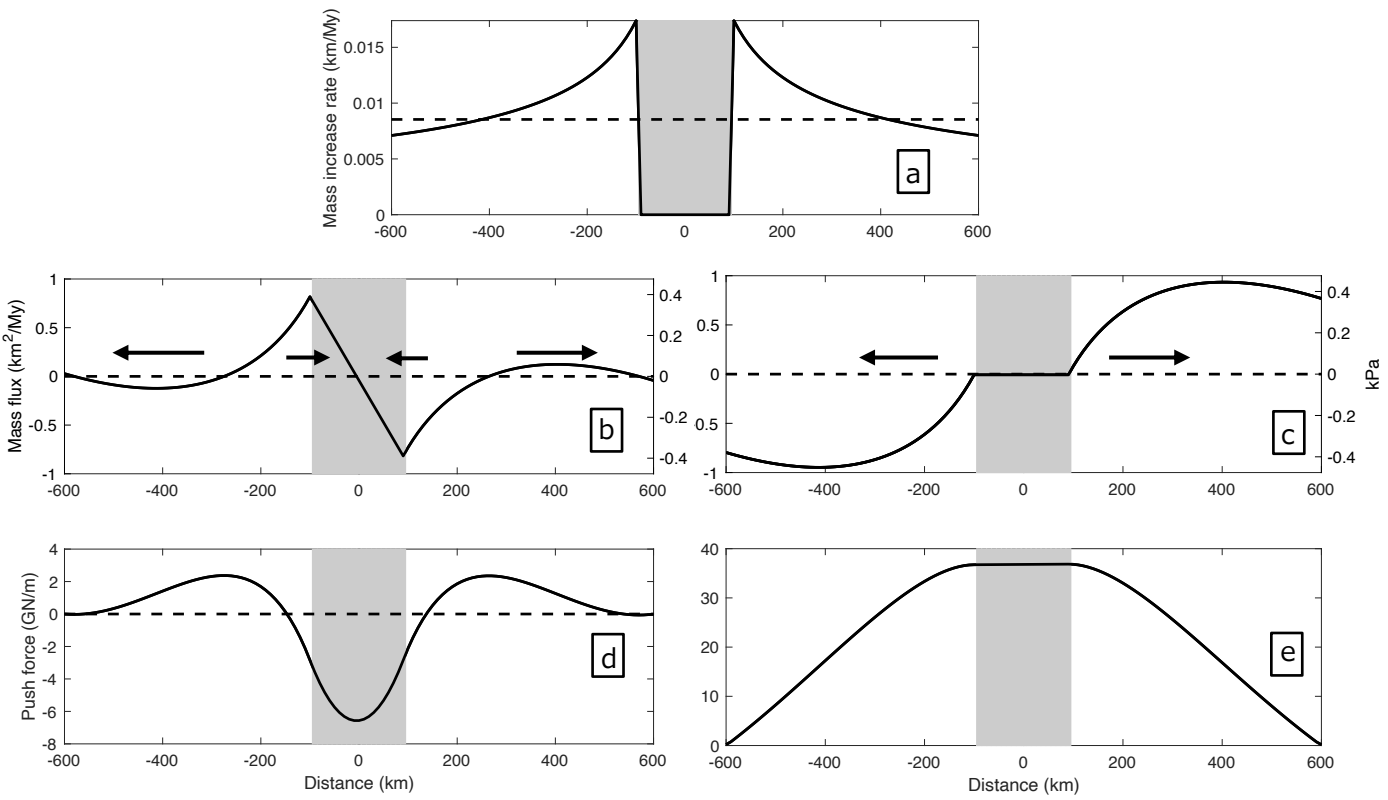


Figure 10

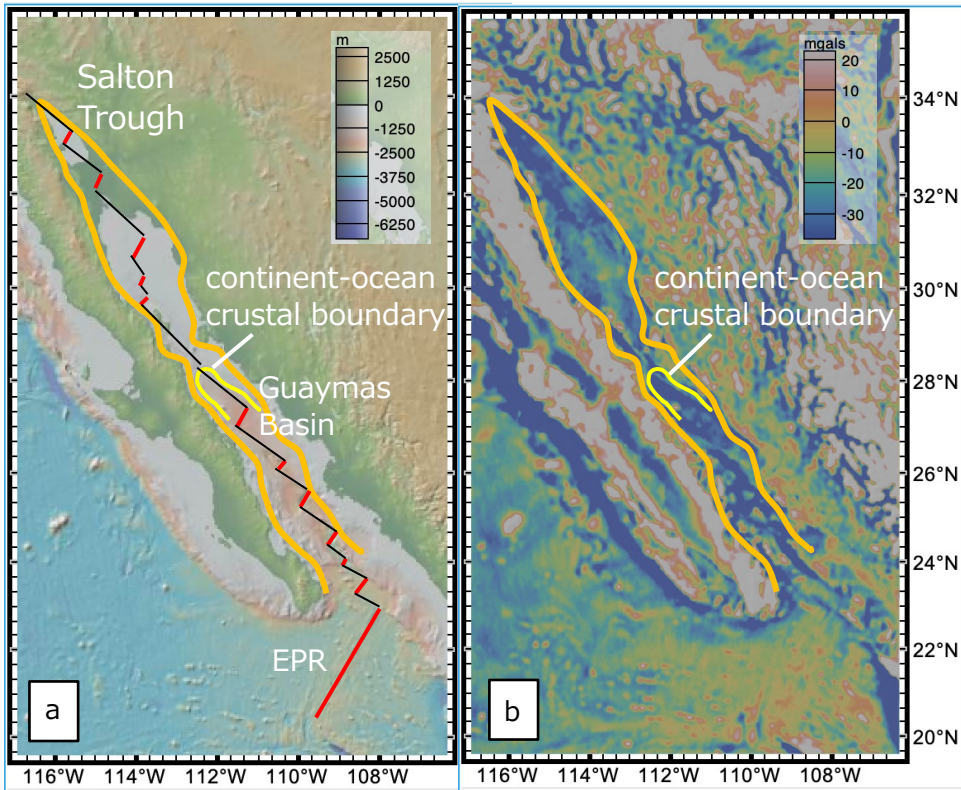


Figure 11

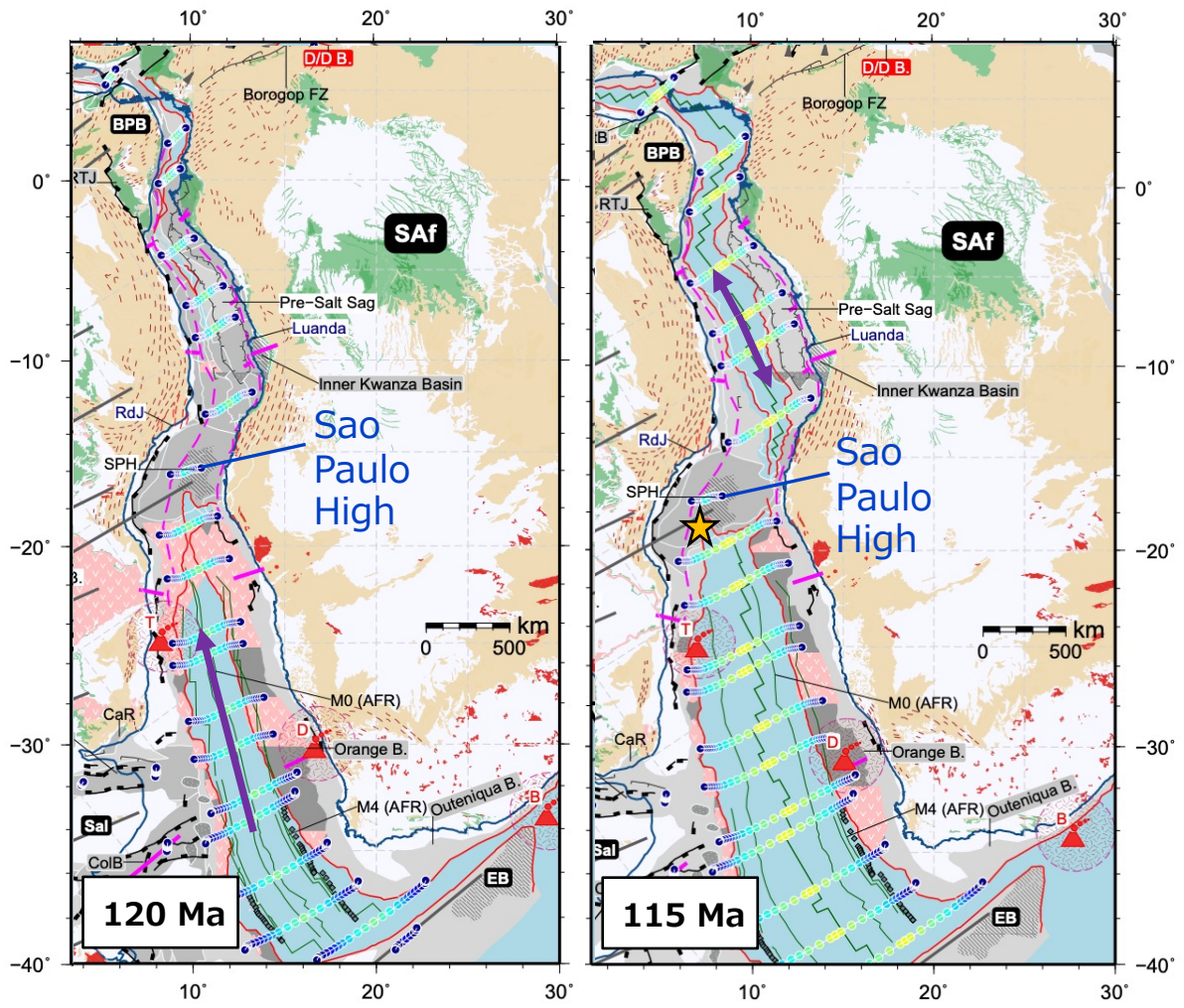


Figure 12

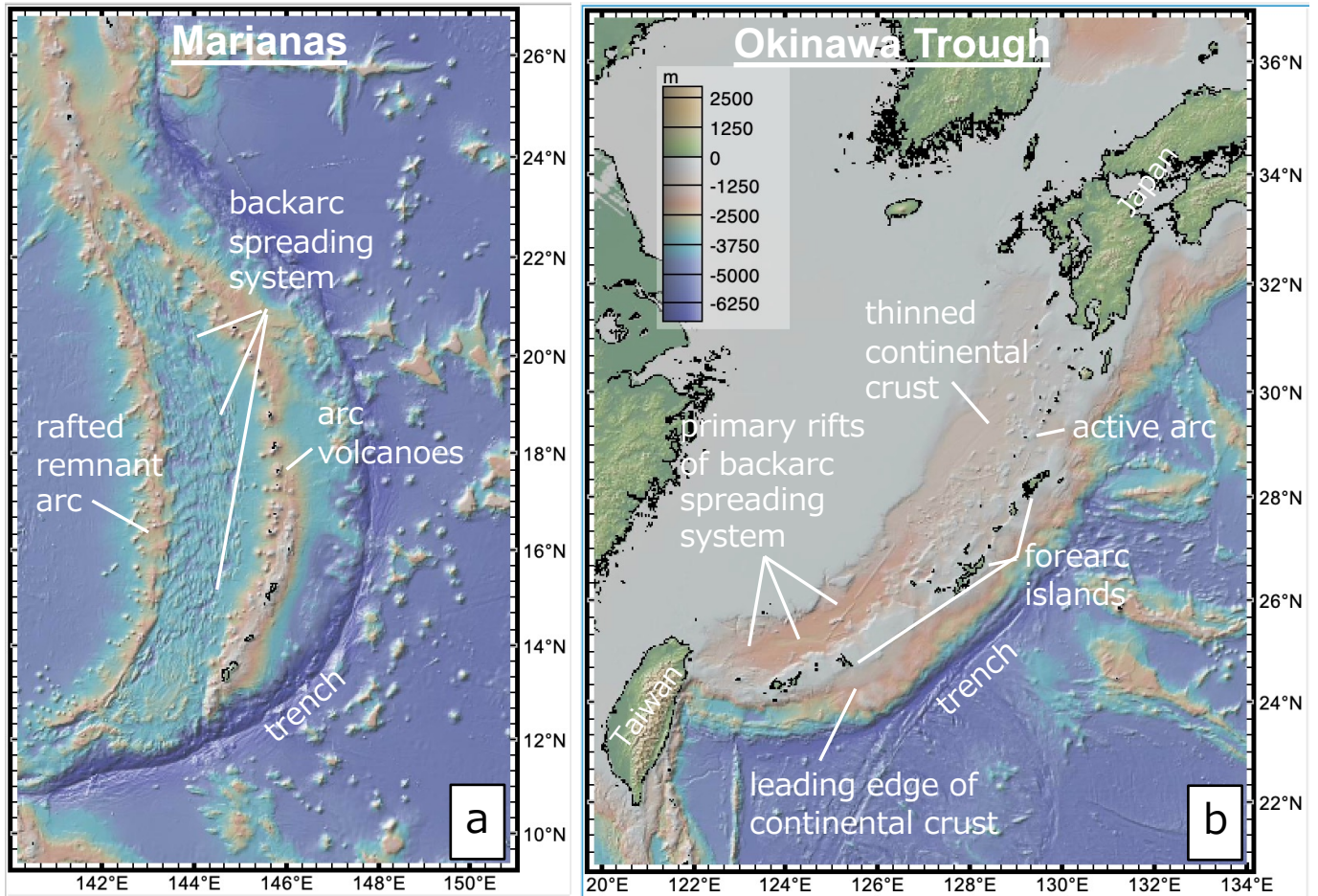


Figure 13

